AN ABSTRACT OF THE THESIS OF

David Shielee for the degree of Master of Science in Mechanical Engineering presented on March 22, 2007

Title: Simulation-Based Micro-scale System Modeling and Design Optimization of a Portable Absorption Cycle Cooling System (Tactical Energy System) Under Uncertainty

Abstract approved:

. .

Ping Ge

Product design is often driven by customer needs and desires. In this case the customer is the US military, and the desire is to have a cooling unit small enough and light enough to incorporate into hazard suits for use in desert combat. The Micro technology-based Energy and Chemical Systems (MECS) being developed at Oregon State University (OSU) and other institutions can generate an extraordinary rate of heat and mass transfer capabilities. As this MECS technology is progressing into the application stages, simulation-based design optimization models will provide invaluable information; saving time and money by guiding the direction of prototype creation and validation. This project studies a 2 kW cooling load based on an absorption cycle ammonia-water cooling system. The absorption cycle was chosen because it requires much less work input in the compression phase than the standard compression cycle systems, making it more suitable for portable applications.

Using basic principles of robust design methodology to reduce the sensitivity of the system performance to changes in input conditions, a more robust system is implemented throughout the research. Specifically for the cooling system that means

that varying ambient conditions and thermal configurations will have less of an impact on overall system performance and system weight. The thermodynamic system modeling is done using Engineering Equation Solver. A tradeoff study is conducted to determine an appropriate design space, and then a D-Optimal fractional factorial design is selected using Matlab to define a manageable sized data sample within the design space with the eight design variables with five levels each. Based on the EES-based thermodynamics model and sizing results, S-PLUS is the statistical analysis program used to develop the surrogate models of the system performance and weight. Microsoft Excel's "solver" function was used to optimize and do a sensitivity analysis of the objective function that was created. The results of this process are a range of potential optimal configurations for the system that can be evaluated and selected by a user depending on conditions and the importance of certain factors. The optimization process generated optimal values for the thermal properties of each component based on a range of starting points. Each of these sets of optimal points had a variance of less than 20% when the input parameters were varied in a range of 10%. The resulting data supplies potential users with a good range of reasonable configurations for a 2 kW system that operate within acceptable parameters.

Simulation-Based Micro-scale System Modeling and Design Optimization of a Portable Absorption Cycle Cooling System (Tactical Energy System) Under Uncertainty

by
David Shielee

A THESIS

submitted to

Oregon State University

in partial fulfulment of
the requirements for the
degree of

Master of Science

Presented March 2007
Commencement June 2007

Master of Science thesis of David Shielee

presented on March 22, 2007.

APPROVED:

Major Professor representing Mechanical Engineering

Head of the Department of Mechanical Engineering

Dean of the Graduate School

I understand that my thesis will become part of the permanent collection of Oregon State University libraries. My signature below authorizes release of my thesis to any reader upon request.

David Shielee, Author

TABLE OF CONTENTS

Page

TABLE OF CONTENTS (Continued)

Page

LIST OF FIGURES

Figure Page

LIST OF TABLES

ACKNOWLEDGEMENTS

First I would like to thank the ME department and OSU as a whole for facilitating my research and providing a quality graduate education. Thanks to my committee for being willing and available to work with me at this critical time in the process.

For their invaluable assistance and oversight of my research, I would like to thank both Dr. Kevin Drost and Dr. Ping Ge. Additionally I would like to emphasize how much I appreciate Dr. Ge's guidance and encouragement at every step in the process as my advisor. She made this all possible

Thanks to my colleagues at PNNL for their collaboration and DARPA for funding the initial steps in my research. I would also like to thank the ME department again for offering a TA position after my funding fell through so that I could continue my work.

A big thanks to all of my friends at OSU who made graduate school a great experience, especially Gabe, Sushim, and Peter. And Thank you to Yuming Qiu for advice and help with a few of the software programs I had to learn to use.

Finally, I want to thank my family for their encouragement and support ever since I decided to get my Master's Degree. You all gave just the right amount of support and necessary distractions to keep me sane through the process.

And to my wife, Lisa. I truly appreciate your willingness to put up with the long nights in the office, and the dinners you had ready when I got home. You are a wonderful wife and I couldn't have done this without you by my side. I love you

Simulation-Based Micro-scale System Modeling and Design Optimization of a Portable Absorption Cycle Cooling System (Tactical Energy System) Under Uncertainty

Chapter 1 Introduction

1.1 Why develop a micro-scale cooling system?

When the ability to cool air below ambient conditions was first developed it did many things for society. It allowed the cooling and freezing of perishable foods, the preservation of special documents and the storage of medical substances, not to mention cold drinks in the summer time. Cooling systems also made working and living conditions more comfortable, but above all of that, they made it possible to populate inhospitably hot climates. Since deserts cover about one fifth of the earth's surface [1], having the ability to use desert regions for expansion greatly increases the livable space on the planet.

The ability to cool a building or large space has been around more than a hundred years, but it has always needed large and heavy equipment to make it happen. Just as cooling systems allowed expansion into desert climates, new micro-scale technology is facilitating the advancement of hi-tech operations in those same environments. The development of micro-scale cooling systems is the next logical step for the field of refrigeration. Currently research is underway to create a micro-scale cooling system that is small, lightweight, and portable.

1.2 Significance and impact

The US military has commissioned projects to create cooling systems small enough to be carried by individual soldiers for specialized use in desert combat. A

portable cooling system built into a protective radiation or chemical suit would allow soldiers to not only survive in contaminated environments, but to carry out missions in relative comfort. Soldiers wouldn't last very long wearing a quarter-inch thick rubber suit in 120 degree weather before heat exhaustion and dehydration became significant issues.

While the military is the driving force behind the research, portable cooling systems could have many other uses, from firefighters or power plant technicians working in high temperature environments, to school mascots dancing around and doing gymnastics under layers of costumes in the heat of summer. They could also be used to provide energy-efficient temporary cooling for transportation and facilities. Once this technology has matured to the commercialization stage it will open all sorts of doors that were previously kept closed by the unmanageable size and weight of traditional cooling systems.

1.3 Ammonia-water absorption cycle

This project will focus on the modeling and optimization of a micro-scale absorption cycle cooling system. A standard configuration for an ammonia-water absorption cycle will be used. Various computer modeling and simulation software programs will be used to simulate and optimize the overall system characteristics to meet certain customer requirements. The load for the cooling system will be 2 kW. The thermal modeling of the system will be done in Engineering Equation Solver (EES), the micro-scale devices' sizing and weight calculation will be carried out in a

stand-along simulation, i.e., SizingApp (part of the modeling task of this project); and system optimization will be implemented in Microsoft Excel.

Previous research has been conducted using a smaller load, (150W) and different modeling software, (ABSIM) [2], [3]. These works formed the basis for this project. The previous work will be discussed in detail in Chapter 2.

1.4 Project Objectives

1.4.1 Objective 1: Conversion to new thermal modeling software

The first step in this research was to model the micro-scale cooling system being considered in a new thermal modeling program, EES. Once a comparable model was generated, it would be necessary to compare the new model with the existing model in ABSIM to prove the accuracy of the EES-based model. Once the new model was validated, making it compatible with the available design tools for optimization was necessary. The details of this process are described in Chapter 3.

1.4.2 Objective 2: Adaptation and improvement of current sizing software

A design tool (SizingApp) was available for sizing the micro-scale thermal devices and calculating the system weight using the existing ABSIM model. Since the new thermal modeling software (EES) was used to replace the ABSIM models, it was necessary to adjust the design tool to be compatible with the new EES-based thermal models. In the process of adapting the design tool, a number of areas were discovered

where it was possible to improve the quality of the current version. This process of adapting and improving the design tool is detailed in Chapter 4.

1.4.3 Objective 3: Conducting simulation-based optimization design

Once valid EES-based models and their compatibility with SizingApp was achieved and processed, the optimization of the overall cooling system was considered. The EES-based thermodynamics models are jointly used with the improved SizingApp in exploring a feasible design space based on extensive tradeoff studies. Because of the highly nonlinear nature of the design space, a Response Surface Methodology (RSM) was considered for a simulation-based optimization design of the targeted thermal system. Using standard Design of Experimentation (DoE) and quadratic model fitting techniques, the high-quality surrogate models for the highly nonlinear design space was generated. The surrogate models evaluate the objective functions (system weight and thermal efficiency, i.e., CoP), and a multi-objective optimization model is then constructed with robustness considerations. The optimization algorithm and the sensitivity analysis of the optimal design(s) were implemented in Microsoft Excel's Solver. This process will be described in details in Chapter 5.

Chapter 2 Background

2.1 Absorption cycle

2.1.1 Basics of Absorption cycles

According to the Air-Conditioning and Refrigeration Institute (ARI), absorption cycles are considered non-traditional refrigeration cycles [4]. Absorption cycles have certain features in common with the standard vapor-compression cycles, but differ in two major aspects [5].

First, the nature of the compression process is different. In a vapor-compression cycle, a vapor is compressed between the evaporator and the condenser. In an absorption cycle, the vapor is absorbed into a liquid (absorbent) to form a liquid solution. That solution of the vapor and the absorbent is then pumped to the higher pressure. Since the specific volume of the liquid is much smaller than that of the vapor, significantly less work is required for the absorption cycle.

The second major difference between the two types of cycles is tied in with the first. Since the vapor is absorbed into the absorbent, it is necessary to then remove the refrigerant from the liquid solution before it reaches the condenser. This requires heat transfer from a high temperature source. For this project, the high-temperature source is assumed to be exhaust gas coming from a burner fueled by natural gas or diesel fuel. The heat is transferred from this source into the liquid solution, and since the

refrigerant has a lower boiling point than the absorbent, the refrigerant boils out of the solution into vapor.

2.1.2 Types of absorption cycles

The two most common types of absorption cycles are lithium bromide-water cycles and ammonia-water. In a lithium bromide-water cycle, the water is actually the refrigerant and the lithium bromide is the absorbent. In an ammonia-water cycle, ammonia is the refrigerant and water is the absorbent. This paper focuses on an ammonia-water cycle. A basic diagram of the ammonia-water absorption cycle used for this project is shown in an EES diagram in Figure 1.

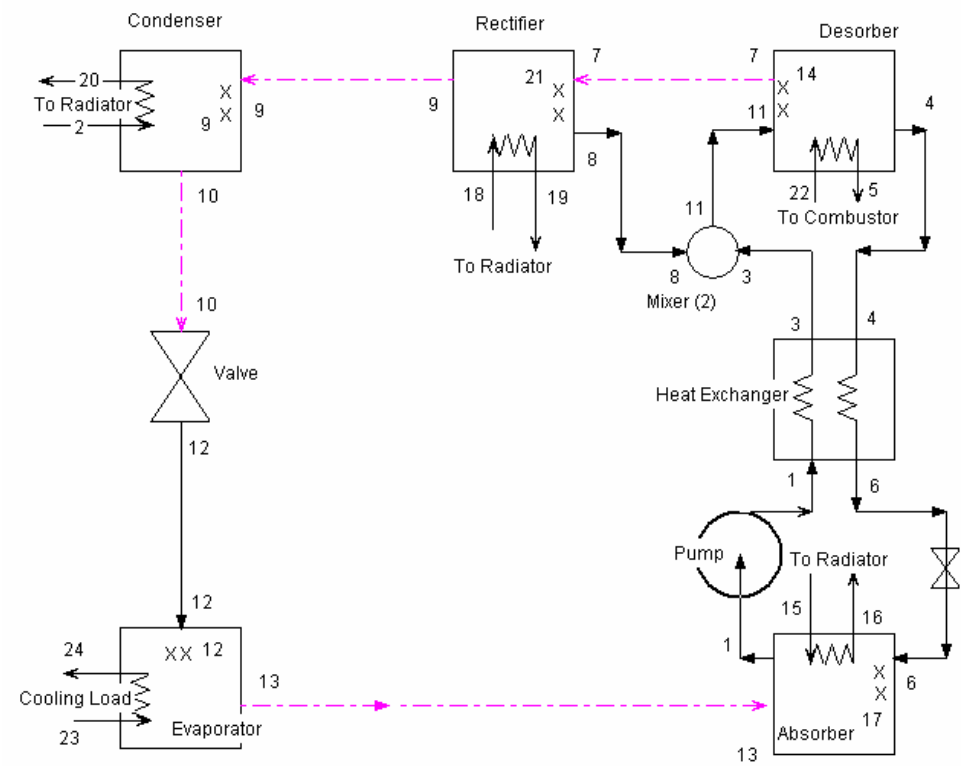

Figure 1 – Basic Absorption Cycle Diagram (EES)

2.1.3 Absorption cycle components

As seen in Figure 1 the absorption cycle used has six main components; the Condenser, the Evaporator, the Absorber, the Heat Exchanger (HEX), the Desorber, and the Rectifier. There are also a few secondary components in the valves, pump, radiator and mixers, and for the sake of vocabulary, each point where the fluids reach a new set of thermal properties is called a "state point" and is denoted by a number.

Starting arbitrarily at state point 1 we have a cold liquid mixture of ammonia and water that gets pumped from the low to high pressure level (all components operate at one of two pressure levels). This mixture enters the Heat Exchanger which simply transfers heat from the hot stream passing through (state points 4 to 6) to the cold stream (state points 1 to 3). After leaving the HEX, the fluid enters a mixer that combines two different flows.

The output from the mixer enters the Desorber at state point 11. The Desorber takes in heat from the external heat source and vaporizes most of the ammonia in the mixture. This ammonia vapor leaves the Desorber and enters the Rectifier. The now low-concentration water-ammonia mixture left in the Desorber exits and is sent through the high temperature stream of the HEX, giving up its energy, before flowing into the Absorber.

The Rectifier takes the vapor that left the Desorber and rejects heat out to the radiator. As the high ammonia concentration vapor rejects heat, the water returns to a liquid state and is removed into the mixer at state point 8; leaving an almost pure ammonia vapor to exit the Rectifier.

The ammonia vapor then enters the Condenser where more heat is rejected and the vapor returns to a liquid. The temperature in the Condenser stays constant; the heat rejected is purely from the phase change from vapor to liquid. The liquid leaving the Condenser then passes through a throttling valve which drops it from the high to the low pressure level, also reducing the temperature.

The mixture then enters the Evaporator where heat is absorbed from the cooling load, and the liquid is vaporized. That ammonia vapor leaves the Evaporator and enters the Absorber, along with the low-concentration ammonia-water mixture that had passed through the HEX. In the Absorber, more heat is rejected to the radiator, and the ammonia vapor from the Evaporator is reabsorbed into the low ammonia concentration solution. The resulting high ammonia concentration solution then leaves the Absorber, returning to the beginning of the explanation.

The absorption cycle is entirely self-contained, with only heat being transferred to and from the components. The Absorber, pump, HEX, Desorber and Rectifier replace the traditional vapor compressor found in compression cycle cooling systems, while the Condenser, valve and Evaporator operate on the same principles.

2.1.4 Component Configurations

Additional aspects of system design under consideration are the geometric configuration of the micro-channels within each individual component, and the system configuration in conjunction with the radiator that removes heat from several components.

Specifics on micro-scale technology will be covered in section 2.2, but Figures 2 and 3 clearly show the configurations of the channels for fluid flow.

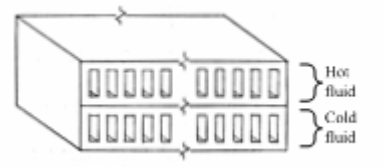

Figure 2 – Channel to Channel Component Geometry

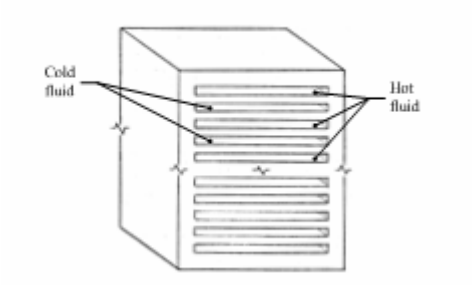

Figure 3 – Interleaf Component Geometry

In Figure 2, for the channel to channel geometry, hot fluid flows in through the top channels, and cold fluid flows through the bottom channels, with the heat transfer happening through the central divider. In Figure 3, the hot and cold channels are interwoven hot then cold then hot again with heat transfer taking place between each channel.

With the differences in radiator configuration the components are actually unaffected other than a difference in temperature. The only thing that changes is how three of the components are connected to the radiator. The Condenser, Absorber and Rectifier are all connected to the radiator. Figure 4 shows the configuration for when they are connected in series.

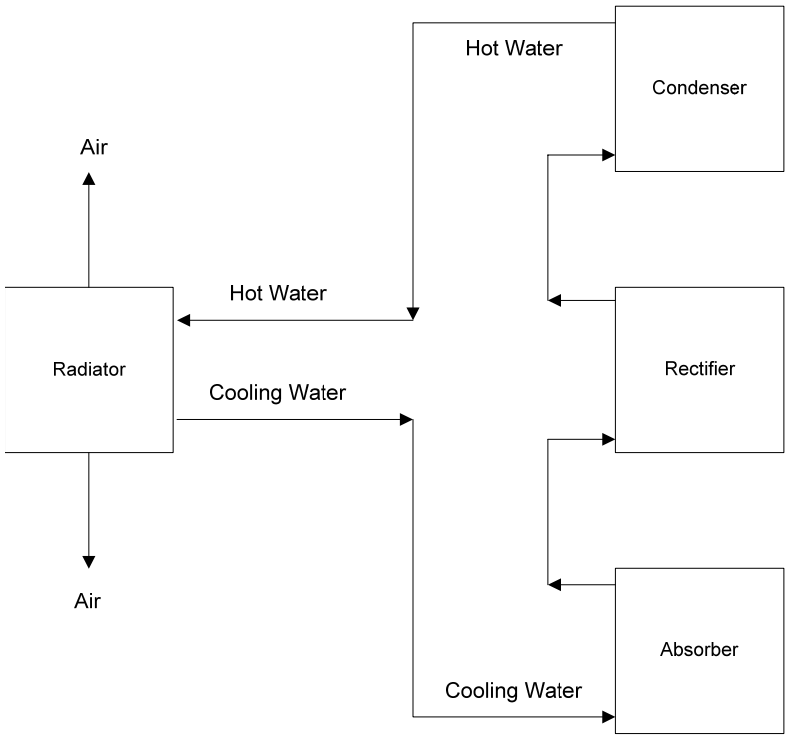

Figure 4 – Series Radiator Configuration

As figure 4 shows, while connected in series, the cooling fluid, in this case water, flows one component at a time through the entire system. As it passes through each component, the coolant temperature rises, making it so that the three different components have three different heat rejection temperatures.

Figure 5 shows the radiator connected in parallel, where the coolant stream is split into three parts, and each component receives coolant at the same temperature. With this configuration, all three components are able to reject heat at the lowest temperature.

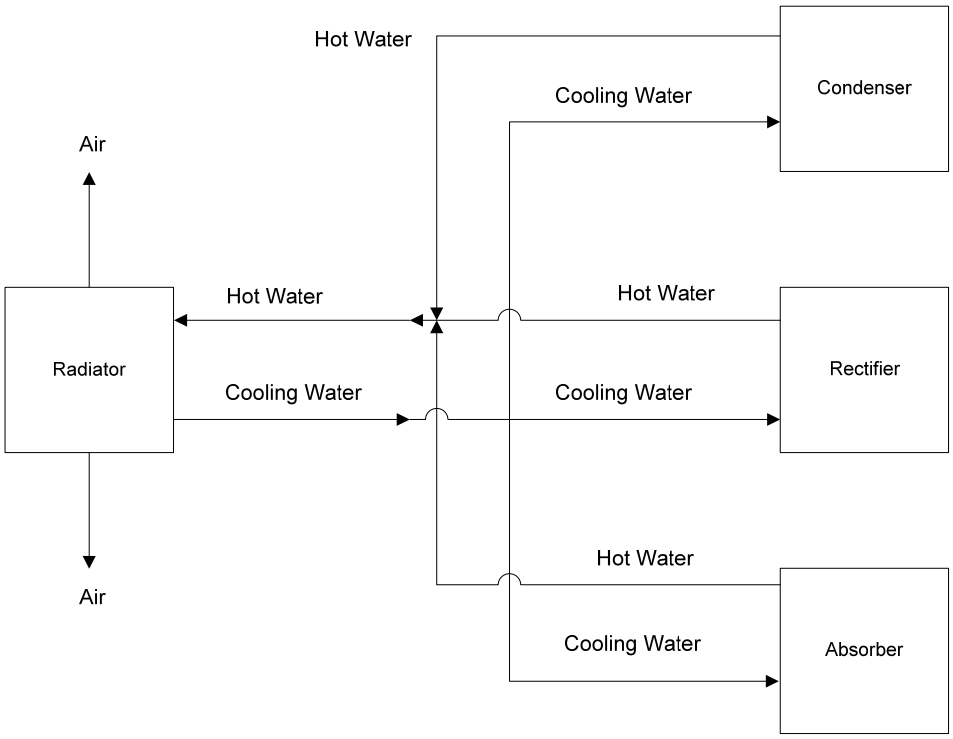

Figure 5 – Parallel Radiator Configuration

2.1.5 Thermal Simulation Software

Absorption cycles, like many other physical phenomenon, can now be analyzed using simulation software. The analysis software also includes the storage of vast numbers of thermodynamic property tables and experimental data. Numerous software packages are available that combine these tables/data with equation solving and programming capabilities to generate computer models for complex thermodynamic systems. In this work, three relevant programs will be discussed and will be described in more detail later: ChemCAD, ABSIM and EES. All three programs have access to large amounts of thermodynamic data, tables and references

that make them powerful tools in computer-aided analysis and design of various thermodynamic systems.

2.2 Micro-Scale Technology and Related Work

2.2.1 Overview

It might go against the common thinking that bigger is better, but when it comes to portable cooling systems and technology in general, smaller is better. NASA, the US ARMY, and industry development companies are all trying to create a portable cooling system as small as possible. Millions if not billions of dollars have been spent researching micro-scale technology. At Oregon State University (OSU), as well as several other institutions, there are micro technology research centers, specializing in Micro technology-based Energy and Chemical Systems (MECS). MECS is focused on applying micro-scale technology to energy, chemical, biomedical, and biological systems. Systems based on MECS technology exhibit extraordinary rates of heat and mass transfer capacity ("heat flux") associated with micro-scale heat exchangers. Researchers at OSU, Pacific Northwest National Labs (PNNL) and other research institutes are beginning to make significant advancements which allow the design, testing, and assembly of several micro-scale thermal devices into a complete portable cooling system [6].

The exciting part about the micro-scale cooling technology progressing to the point where prototypes are being built and tested is that researchers will soon have the ability to not only theorize and run simulations to suggest possible results, but they

will be able to run simulations, then run tests, and compare the theoretical and empirical data to search for optimal system design.

2.2.2 Related work to this project

A previous graduate student at OSU, Brian Daniels, conducted a research project on the thermal analysis of individual components of a portable micro-scale cooling system (2003). He generated first principle-based, theoretical models for multiple configurations of the individual components for a micro-scale absorption cycle cooling system [1]. A collection of additional research that has been conducted in this area was put together by Ashutosh Ballal [2].

The micro-scale condensation phenomena required in condensers and absorbers has been investigated by Koyama et al.[7], Kim et al.[8], and Cavallini et al.[9]. The boiling phenomenon of single species refrigerants and binary mixtures present in evaporators and desorbers at the micro-scale has been studied by Steinke and Kandlikar [10], Koo et al.[11], and Zhang et al.[12] Pumps have been developed by several researchers [13,14,15,16]. A micro-scale combustor has also been developed by Drost et al.[17]. The feasibility of a complete heat-actuated cooling system has been theoretically investigated by Drost and Friedrich [18], Drost et al.[19] and Munkejord et al.[20]. Drost, Friedrich and Munkejord all investigated a vapor compression style cooling system, however the feasibility of this style cooling system is limited by the need for a vapor compressor, and a micro-scale version of which has not yet been developed. Drost et al.[19] examined a water/lithium bromide absorption cycle system.

Daniels' theoretical thermal models were the basic building blocks for SizingApp, a software design tool that was then created by Ballal (2004) to size each component of the cooling system. SizingApp applies the theoretical models to each of the components in an absorption cycle (simulated by a stand alone thermal modeling software: ABSIM). It sizes each of the components and then calculates the theoretical weight of the whole system. This original design tool, SizingApp, is what I have modified, improved, and then used to generate data for the optimization analysis in my research project. The specifics of how SizingApp works and the details of what it DoEs will be explained in more detail in Chapter 3.

2.3 Response Surface methodology

For many real world optimization problems, it is necessary to consider Response Surface Methodology (RSM), because the nature of the design space (mathematically expressed as a mapping relationship between the performance and design variables) is unknown. Even when existing physics principles can be used to explore the design space, the physics principles-based equations are usually highly nonlinear, and may render an explicit math expression of the design space unattainable as it is in this research project. It is therefore necessary and suitable to adopt a RSM approach. RSM is a collection of statistical and mathematical techniques used for developing, improving and optimizing processes [21]. For this research project, four steps are implemented in the RSM approach, including 1) conducting a tradeoff study to explore the scope and characteristics of the highly nonlinear design space; 2)

collecting data from computer simulations or physical experiments using Design of Experiment (DoE) techniques for surrogate model construction [22], 3) building high quality surrogate models of the highly nonlinear relationships of the design space [22], and 4) combining the surrogate models and tradeoff study results in a optimization model to search for an optimal design.

It is always helpful to break down an intricate design space into smaller sections (or sub-spaces) for investigation and then determine a feasible design space in which to focus the optimal search. By conducting a tradeoff study, it became clear for this project what ranges are appropriate for each important design variable, resulting in a more focused design space, where possible optimal solutions lie.

One common form of DoE involves 2^k factorial designs, where k number of factors have 2 levels each. Often, when a quadratic fit for the model is desired, a third or "axial", point is used to increase the accuracy. There are also fractional factorial designs. When the number of factors involved in a simulation increase, the number of runs required for a complete replicate of the design also increases. For example, a complete replicate of a 2^6 factorial design requires 64 runs. In comparison, a 2^7 factorial design requires 128 runs [21]. And that is only using two levels for each factor. Fractional factorial design takes well established and researched combinations of levels and factors and focuses on terms within the interaction that are known to be important. This allows for a reduction in the number of runs required to generate a quality model. A form of this fractional factorial design will be implemented in the DoE for this project in generating the surrogate model.

This project's design space is modeled using the design variables as factors, and the system weight data generated by SizingApp as the output. That data will then be analyzed in the software program S-PLUS and a surrogate model will be generated. S-PLUS is a powerful data analysis package that will be explained fully in Chapter 5.

2.4 Optimization in Engineering Design

Once the surrogate model is generated in S-PLUS, the task will be to optimize the overall system design. That will involve evaluating, comparing and altering the design variables and therefore the outputs to create the most efficient system configuration. The outputs to be optimized for this system are the coefficient of performance (CoP), and the system weight. The optimization process will create an objective function that includes both of those terms and give them determined levels of importance in order to create the best possible system. Several programs exist that have optimization abilities, but Microsoft Excel has a "solver" function that will be utilized to perform the actual optimization process for this project. The details of how Excel's solver works will be described in Chapter 5.

2.5 Robust Design

Genichi Taguchi [23] first used the term robust design. Taguchi proposed a procedure to take the variations in system performances into account. He introduced the concept of parameter design that improves the robustness by reducing the sensitivity of variations in system performance. In this case, the goal is to make the cooling system robust to changes in climate and operating conditions, and control the

variations in weight and system performance. Using this robust design methodology the goal is to find an optimum design point that not only maximizes the system thermal efficiency and minimizes weight, but also reduces the overall sensitivity of the system. Robust design methodology will be incorporated into the objective function.

Multi-objective optimization techniques are widely adopted for implementing a robust design methodology. For a multi-variable design problem, it is necessary to adopt an optimization model to determine where the optimal performance is, given numerous possible varying inputs. When more design variables are added, the optimization model and process can become significantly complicated. Making it a robust design complicates things even further.

Chapter 3 Thermodynamic Analysis

3.1 Absorption cycle modeling using ABSIM

3.1.1 A Brief Description of ABSIM

As described previously, the original thermal modeling on this project was done using an Absorption SIMulation program (ABSIM). ABSIM is modular in nature, and generates thermal/chemical cycles by linking several modules together that represent different components. Figure 6 shows one example of a cycle that had been used for previous work [3].

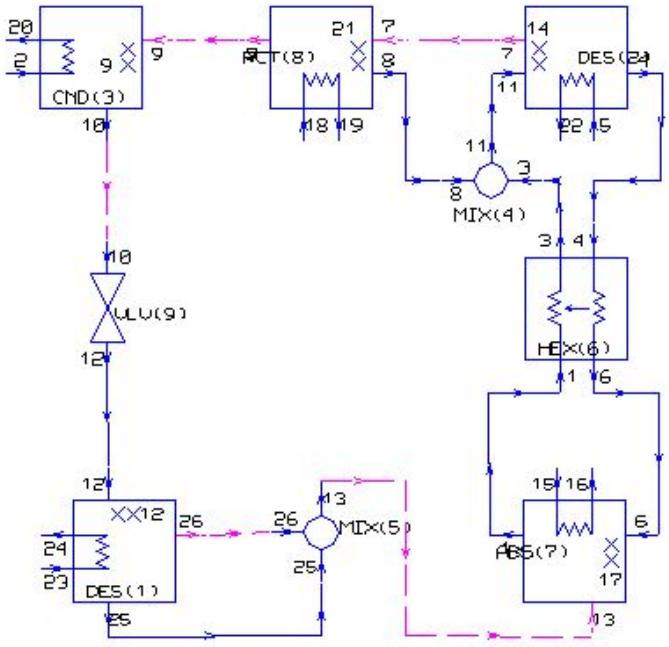

Figure 6 – ABSIM Diagram

Once the components for the absorption cycle are properly linked together and certain state point data is input, ABSIM simulates the cycle using data from standard charts through an iterative process to achieve a heat transfer balance in the cycle. It returns the flow rates and various thermodynamic values at the inlet and exit of each component.

3.1.2 Strengths of ABSIM

ABSIM is a very powerful program. It has the ability to process large numbers of calculations and variations quite quickly. All of the necessary thermodynamic properties are stored within the program, and one of the most useful features is that ABSIM already has the basic components of most heat pump/absorption cycles preprogrammed as components (i.e., modules) that can be easily used in the integration and design of systems.

3.1.3 Problems with ABSIM

While ABSIM is powerful and is accepted by the thermodynamic community as being accurate it does have some negative aspects. Fist of all, ABSIM is a black box type program. The user supplies certain inputs, runs the simulation, and then ABSIM gives outputs. It is not transparent to the users how values are achieved, or what principles govern the process. Secondly, ABSIM is not as robust as desired in its operation. At times, it can be very difficult to get to converge on an answer, in which cases, there is no data given out. Worst yet, it gives no explanation as to the reason it won't converge and no suggestions on which inputs to change to help it converge.

3.2 Shifting from ABSIM-based to EES-based simulation

It was determined by PNNL and the research team at OSU that ABSIM was no longer sufficient to supply the necessary simulation data. A search was initiated to find the best method of simulating the thermodynamic cycle. In the end, Engineering Equation Solver (EES) was chosen as the most appropriate program.

EES was developed by two professors from the University of Wisconsin, for the express purpose of simplifying thermodynamic design problem calculation and data tabulation [24]. The goal of these two professors was to simplify the use of property information and solving equations to speed up the process and allow more time to be spent focusing on cycle design. EES is capable of solving large sets of linear and non-linear algebraic and differential equations. It can also do optimization and uncertainty analysis if desired. One of the most useful features of EES that makes it easier to use than other programs is that it doesn't matter what order the equations are entered in. As long as each variable is designated, set, or solved for at some point in the program, EES is smart enough to solve for it and be able to use it.

3.3 Constructing component- and system-level modeling using EES

3.3.1 Cycle modifications

The ABSIM model that was used in the previous research done in this area used a somewhat improvised absorption cycle. ABSIM was not able to converge when a standard configuration absorption cycle was used. Instead of using an evaporator a second desorber was used and then the two streams from the desorber

were fed into a mixer. When converting this model to EES, it was not necessary to include these modifications, so a more standard absorption cycle was modeled. Part of the reason this was possible is that the EES code is controlled from state point to state point within the components based on standard thermodynamic properties and reactions instead of on a component basis like ABSIM. The EES code is laid out line by line and can be followed step by step through the cycle to verify that the process is correct. The previous absorption cycle shown had the ABSIM modifications included. Figure 7 shows the cycle that was used in EES.

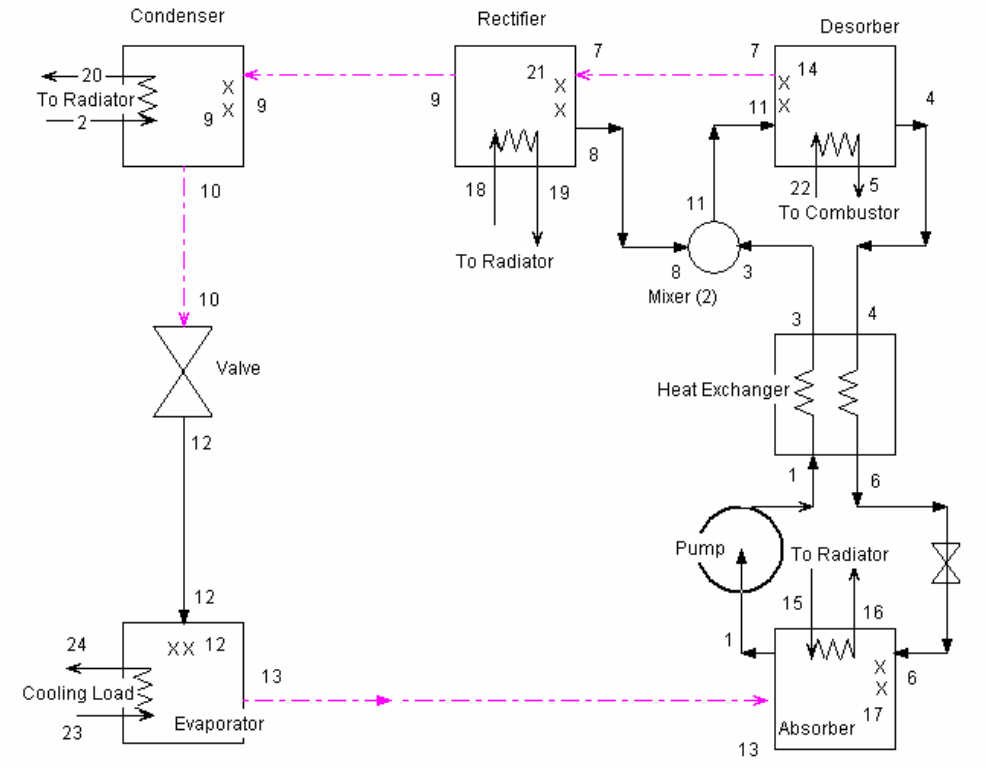

Figure 7 – EES Diagram

3.3.2 Fewer Restriction

The range of the design space used in previous research was confined by the scope of values that ABSIM could use to converge. EES is capable of converging using a much wider range of values. This has allowed a much larger design space to be examined, leading to a more conclusive analysis. Another benefit to EES is that when it encounters an error or unreachable value in its iterative calculations, it will inform the user approximately where the error occurs to make it easier to determine which component caused the error and how to fix it.

3.3.3 Verification of EES thermal model against ABSIM

A study was conducted to verify that the cycles in EES and ABSIM were indeed equivalent. Each of the ABSIM outputs at each state point was recorded. These values were then compared to the matching EES output values. Initially, this made it apparent where a few minor differences existed in the two cycles. These differences were corrected, and then the data was compared again. The EES cycle's CoP was only 1.65% different than that of the ABSIM cycle. The flow rate was off by almost 10%, but that is explainable because in EES, it is assumed that the vapor leaving the rectifier is pure ammonia vapor, and in ABSIM there is some water included that increases the flow rate at several state points. Other than that difference in flow rate, all of the properties evaluated matched within 6 %. It was clear that EES was capable of generating similar data within an acceptable margin of error, and it had additional benefits. One major benefit being that with EES the user can determine the

name and location in which each output file is exported to. The decision was made to move forward with the research using EES as the thermal modeling program.

3.3.4 Generating Similar Output Files

Since the SizingApp software that does the system weight analysis was developed to read from ABSIM output files, it was necessary to match the format of the ABSIM .out files with the EES export files. It was simple enough to match the basic structure and configuration of numbers in the data files, but EES was unable to match the .out files exactly. The EES export files had the data separated by commas as opposed to spaces. It became necessary to modify the SizingApp code to be able to read EES data, but that will be discussed in Chapter 4.

3.4 Comparative study between EES, ABSIM and ChemCAD

Once the model was completed in EES, validated against ABSIM and able to be read into SizingApp, PNNL sent over another cycle that had been modeled using ChemCAD, their program of choice. They requested that the EES model be compared to the ChemCAD model for further validation and verification of accurate results.

3.4.1 Differences in ChemCAD model

The ChemCAD model was slightly different than both the ABSIM and the EES models that had been created to that point. Not only did it use different initial state point values for some of the key components, the mixer and recuperator coming out of the desorber were configured differently. So for the benefit of PNNL, a new

EES model was created to match the configuration of the ChemCAD. Initially a figure showing the ChemCAD model was included here, but the only model available was marked as "Not for public disclosure – DRAFT"

3.4.2 Comparing ChemCAD to ABSIM

Initially an attempt was also made to convert an ABSIM model to match the configuration of the ChemCAD model so that a 3-way comparison could be performed. After much effort was invested in the attempt, ABSIM was unable to converge on a solution with this new configuration. A model that was as close as possible to the ChemCAD configuration was created, and a matching EES model was made to allow a comparison, but it still proved to be significantly different, and the decision was made to ignore ABSIM for the sake of this comparison. Since ABSIM is already recognized as a valid program and has been verified, it was not necessary to prove to PNNL that it was accurate. This decision allowed the study to focus specifically on the comparison between EES and ChemCAD.

3.4.3 Comparing EES to ChemCAD

Using the EES model that had been adapted to match the configuration of ChemCAD, a comparative analysis was performed. A diagram of the modified EES model is shown in Figure 8. A difference in the flow rates due to the fact that EES was assuming a perfect theoretical model reached an almost 4.5 % difference at a few state points as happened with ABSIM, other than that, the differences in property

values between the two cycles was less than 1.5 %. Even the heat balance which accounts for all of the components overall heat transfer was exactly the same.

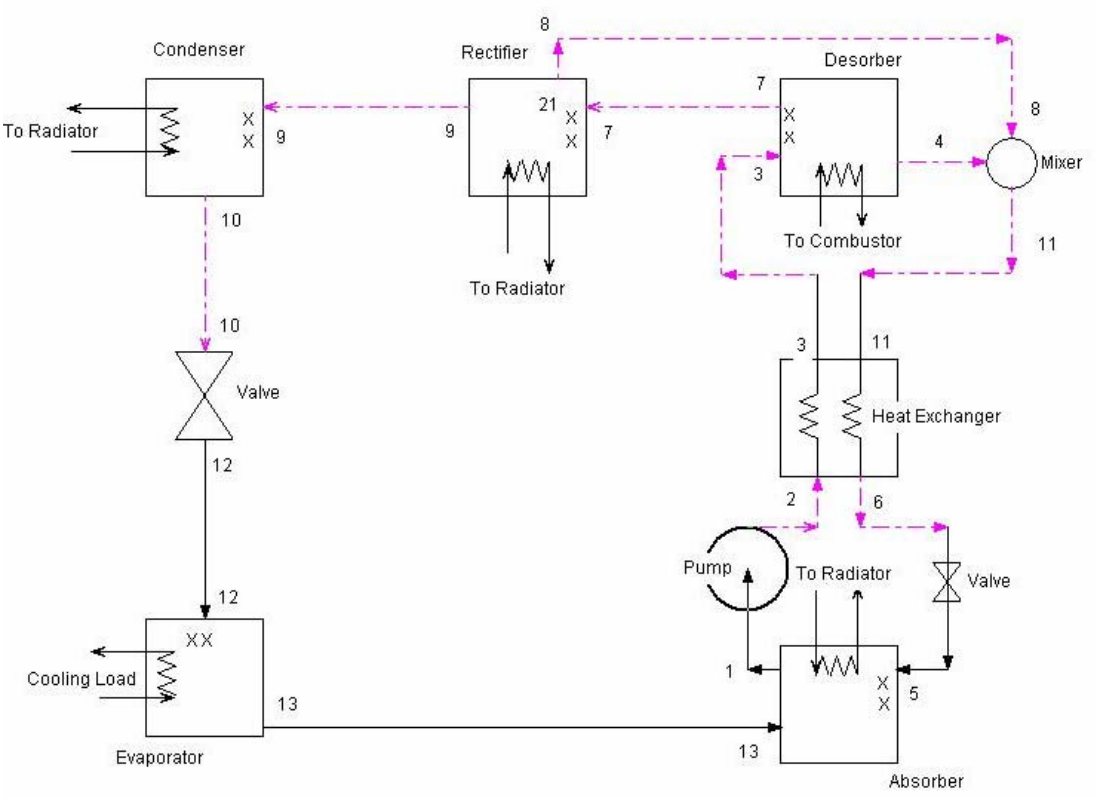

Figure 8 – EES Model for Comparison with ChemCAD

3.4.4 Overall comparison results

The comparisons showed that EES is a very capable and flexible program that is able to match both the ABSIM and ChemCAD models effectively. It is clear that EES is a valid program and is capable of supplying the data and analysis required for this project.

Chapter 4 Improving the Existing Sizing Module

As stated before, the original version of the SizingApp code was developed by Ballal. It is not a commercial software package that can simply be installed and then run in any operating and/or programming environment. The source code files were saved to a disk in standard folders as .class and .java files. It was necessary to adapt these files for the new project in this thesis work. More importantly, EES-based thermodynamic analysis is used to replace the ABSIM-based models for which the original SizingApp code was developed. As a result, several necessary steps were taken for adapting and improving the current SizingApp code.

4.1 Adapting the original SizingApp in the new project

4.1.1 Access Issues with JAVA environments

Initial attempts to access SizingApp were made using the JAVA programming environment Java Workshop 2.0. When these attempts were unsuccessful, the original author of SizingApp, Ashutosh Ballal, was contacted. He shared the information that JCreator was the environment used to create SizingApp. Once JCreator was downloaded, it took some time to become familiar with how to develop and manage JAVA codes in that environment. With much effort, eventually SizingApp was successfully accessed and running.

4.1.2 Converting from ABSIM-based to EES-based Platform

Once SizingApp was up and running, data was generated using stored ABSIM files and compared to previous results to make sure it was operating properly. After verifying that it was indeed generating similar results as before, the attempt was made to read in and analyze the output from an EES-based thermodynamic analysis output file, since EES would be the new platform. However, the EES files were not compatible with the original version of SizingApp (developed by Ashutosh Ballal). It became necessary to modify the SizingApp code in order to make it EES compatible. EES-based thermodynamic analysis output files needed to be read into SizingApp.

For the purpose of adaptation, it was necessary to search through the thousands of lines of SizingApp code to determine where the files are input / parsed; and why the SizingApp program was unable to read the EES output files. After much debugging, it was determined that SizingApp searched the selected data files for a target phrase that indicated where the useful data began. EES was unable to match this target phrase exactly due to the fact that it cannot output strings(words) without a string indicator; in this case, an apostrophe (‘). Therefore, the target phrases were changed in the SizingApp code to match the EES output files. With this modification, the SizingApp started to recognize the target phrases and began searching for data to read, but was still unable to read the EES output file data tables. The ABSIM.OUT files have data separated by spaces, and scientific notation was denoted as 0.00D+00. EES outputs data as comma separated values and has the standard scientific notation of 0.00E+00. It was simple to get SizingApp to read the “E” instead of a “D” for scientific notation.

Additional changes were made to include a comma as a possible delimiter in the code and enable SizingApp read comma separated values. This solution may sound simple, but finding the specific line in the code where this was necessary was like finding a needle in a haystack. Once the problem was located, and the comma added as a delimiter, the modified SizingApp was able to read in EES output files.

4.2 Correcting errors in SizingApp

After the adaptation, much more work was put into improving the SizingApp code in its scientific soundness and operating robustness. It is worthwhile to note that while certain errors were found in the code, it is not entirely clear which problems arose from mistakes in the original code, and which came about during the adaptation process described above. As such, this section should not be seen as belittling previous work and research.

4.2.1 Correction of oversights

It became apparent while searching through the code that certain sections of the original SizingApp program had oversights that could impact the system weight calculation. For example, code had been written that evaluated the size and weight of certain peripheral machinery such as the fan and battery with the evaporator and the burner, fuel and fuel tank with the desorber. In several places this code had been commented out and was not included in the overall system analysis without any explanation. After validating through the theoretical models that the code was

accurate these sections were reinstituted and incorporated into the system weight calculation.

4.2.2 Correction of errors

After becoming more familiar with the theoretical models and java coding, it also became apparent that there had been several mistakes in the code; and not just the previously stated oversights. Several assumptions were made in the original code that were not necessarily accurate, one mistake with units caused a major oversight, and some of the variable names were wrong causing data to be ignored. Due to the space limitation, the rest of these errors are not specified and elaborated here. See Appendix B for a summary list of the specific errors and corrections in relation to Section 4.2.1 and 4.2.2.

4.3 Additional changes implemented

Not only were corrections made to errors and oversights in the SizingApp code, additional capabilities were added to the program. While converting SizingApp to read data from EES, it also became more robust in general in its ability to read data. In addition, the length of the channels within the components was converted from a constant value set in the code, to a value set within the graphical user interface (GUI). This allows the channel length to now be used as an additional design variable, increasing the quality of the optimization model.

Throughout the process of converting SizingApp to read from EES, general adjustments, and correcting errors, all changes made were documented and listed by approximate line number at the end of each file so that verification and tracking of the changes is available in the future. See Appendix B for these lists.

Chapter 5 Simulation-Based Robust Design

5.1 Robust Design Methodology Overview

As discussed in Chapter 2, Taguchi's concept of robust design methodology reduces the sensitivity of a system to changing parameters. For a micro scale cooling system that means minimizing the affect that changing conditions and configurations have on system weight and performance. Considerations for robustness of design were made throughout the research process, but are most notable in the implementation of a sensitivity analysis within the design function. System sensitivity will actually be considered as part of the optimization objective function.

Chapters 3 and 4 walked through the research involving the thermodynamic modeling and the conversion and improvement of the sizing model for capturing the relationship between design variables and system performances, i.e., weight and CoP. This chapter will explain the identification of the design space through use of an extensive tradeoff study, demonstrate how that design space was investigated using design of experimentation, and then finish by covering the data processing method and final analysis. Figure 9 shows a basic flowchart outlining the overall process. The first two components, the thermodynamic simulation (Chapter 3) and sizing of the components (Chapter 4), have been discussed. This Chapter will focus on the next two steps to finish the study.

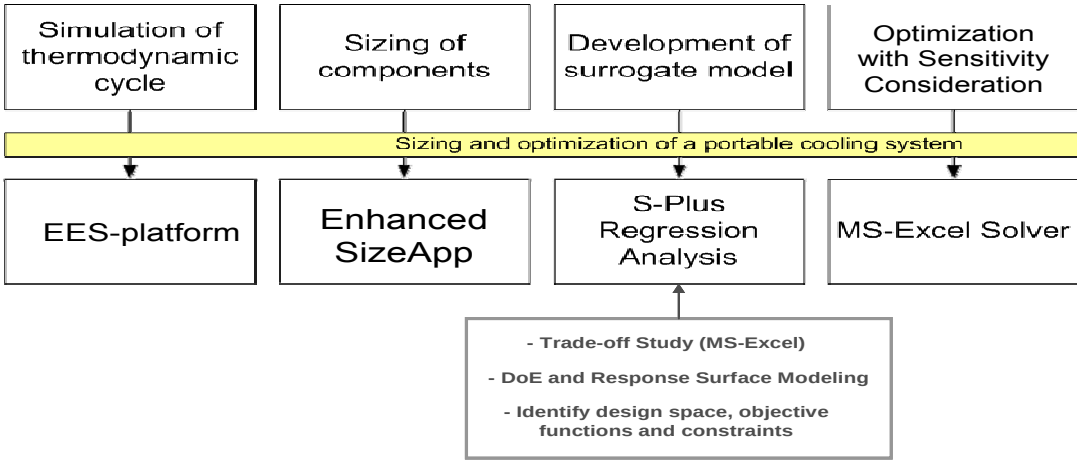

Figure 9 – Flowchart of Design Methodology Overview

The development of the surrogate model is covered in section 5.2 and 5.3. More specifically, section 5.2 will walk through and explain the tradeoff studies and setting the range for the design space. Section 5.3 will give details about using Matlab to create a manageable size for the design space and generating a surrogate model using S-PLUS. Optimization with sensitivity consideration will be addressed in Section 5.4, where the optimization design model will be constructed based on the surrogate model of the system performances obtained in section 5.2 and 5.3. It will be implemented using Microsoft Excel's "solver" function. Section 5.5 will summarize and interpret the results.

5.2 Defining the design space through tradeoff studies

As shown in Figure 9, once the SizingApp code was completed and ready to generate simulation data (Enhanced SizingApp), it was necessary to define the design space within which the surrogate model would be generated for the optimization

design. The variables to be considered, as well as the tradeoff studies to determine each of their ranges, are described and explained in the next few sections.

5.2.1 Design variables and their meaning

Table 1 shows each of the design variables being considered for this project. The first column is the name of the variable, the second column shows its symbol, the third column shows the units used and the fourth column shows the corresponding X representation for use in equations.

Table 1 - Design Variables and Representations

Design Variable	Notation	Units	X Representation
Condenser Temp.	Tcond	deg. C	X_1
Desorber Temp.	Tdes	deg. C	X_2
Absorber Temp.	Tabs	deg. C	X_3
Critical Approach Temp.	CAT	deg. C	X_4
Channel Width	Ch_W	m	X_5
Channel Length	Ch_L	m	X_6
Temp. Hot out HEX	T_6	deg. C	X_7
Low Pressure	P_low	kPa	X_8

Originally there was another variable for the evaporator temperature. Upon initial study of the system, it was determined that the evaporator temperature and the low Pressure level have a linear relationship. When one value was changed, the other value could be predicted with reasonable accuracy. Therefore the decision was made to evaluate only one of these related variables, with the understanding that the evaporator temperature would be a variable constraint within the range of 6.8 to 21.5 degrees C.

5.2.2 Trade off study

In order to determine what range to evaluate the design variables in, a preliminary tradeoff study was conducted. For each variable, thermal models were generated that pushed the limits of convergence to find the maximum range of feasibility. For each of the variable not being considered in the tradeoff study, a mid-range value that was known to work was selected, and then the variable in question was pushed to the limits of where EES could converge. This provided a range in which to focus the optimization process.

5.2.2.1 Condenser

The tradeoff study for the condenser showed that EES would converge while the condenser temperature was within a range of 50 to 110. Figures 10 and 11 show the tradeoff studies for the condenser giving system weight in grams on the left Y axis, and CoP on the right Y axis with Figure 10 showing data for the Series configuration, and Figure 11 showing the Parallel configuration.

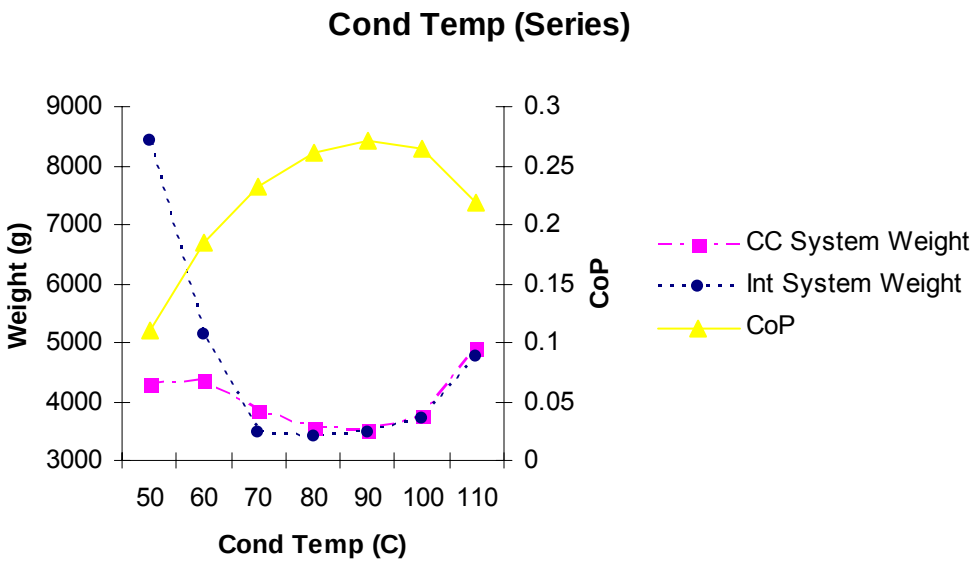

Figure 10 – Condenser Temperature (series)

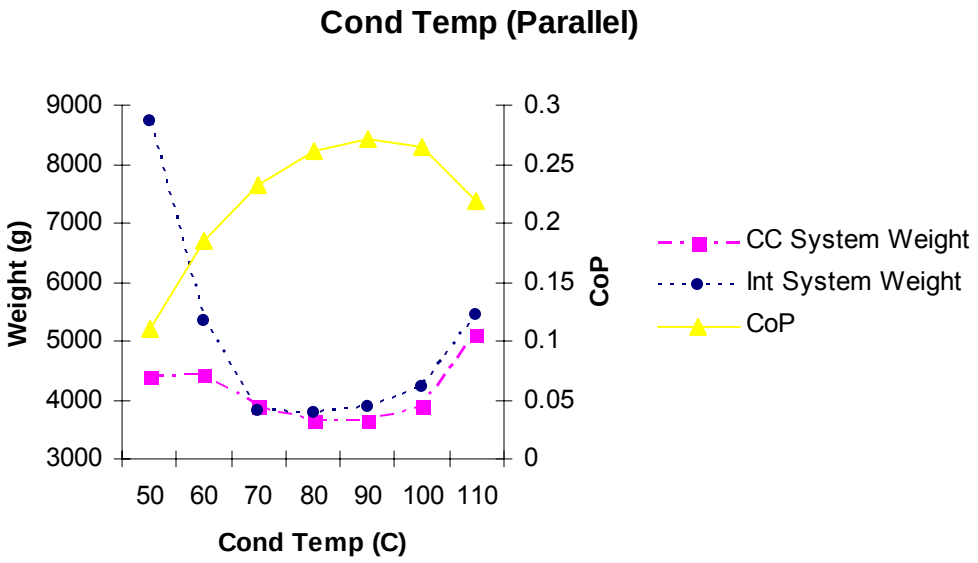

Figure 11 – Condenser Temperature (parallel)

Both graphs show fairly clear trends in system weight and CoP as the condenser temperature changes. The Series configuration appears to have slightly smaller values for system weight, but the curves are very similar. The CoP peaks at

about 0.275 at a temperature of 95 degrees C. At the lower temperatures the CoP drops dramatically, and the interleaf system weight skyrockets. It would make sense for the CoP to increase as the condenser temperature goes up, because it would allow the Evaporator to reject heat more efficiently from the higher input temperature. From these graphs it is clear that the design space should focus on the area between 60 and 100 degrees C.

5.2.2.2 Desorber

The tradeoff study for the desorber showed that EES would converge while the desorber temperature was within a range of 160 to 230. Figures 12 and 13 show the tradeoff studies for the desorber giving system weight in grams on the left Y axis, and CoP on the right Y axis with Figure 12 showing data for the Series configuration, and Figure 13 showing the Parallel configuration.

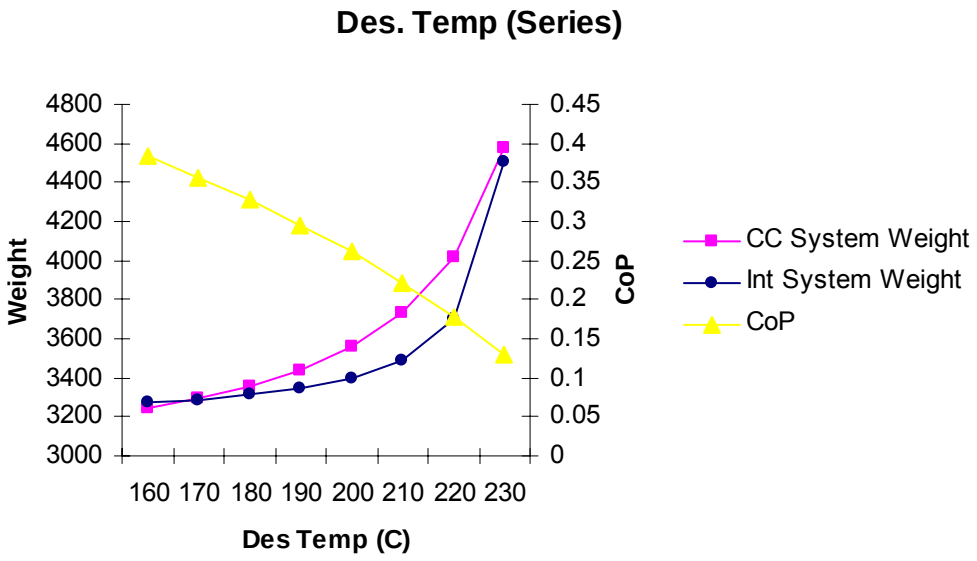

Figure 12 – Desorber Temperature (series)

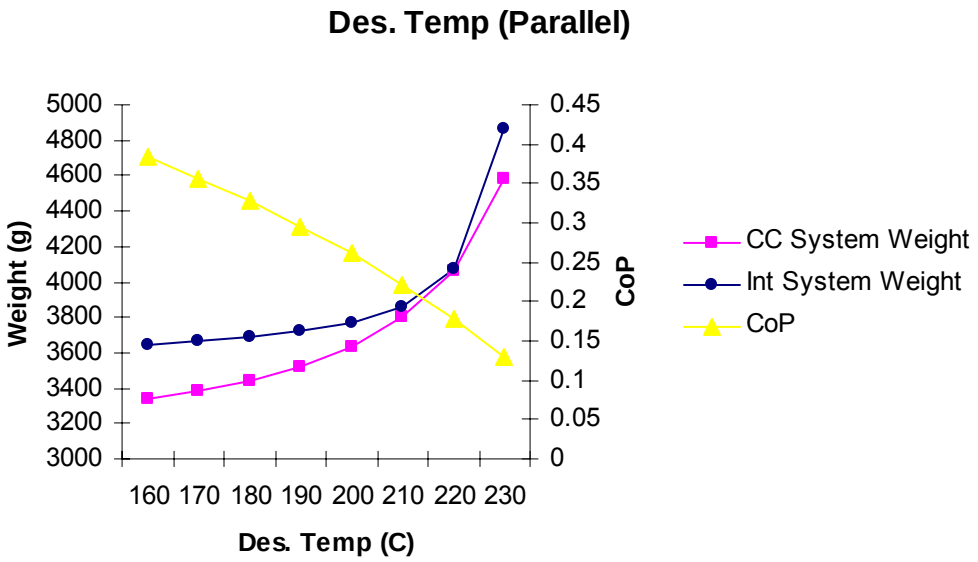

Figure 13 – Desorber Temperature (parallel)

The CoP steadily decreases as the temperature increases, and the system weight shows the opposite trend. This trend is most likely explained by the fact that as the desorber temperature increases, more energy is being input into the cycle, reducing the efficiency and the CoP. With a less efficient cycle, all of the components must work harder, increasing the overall system weight. It is clear that it will be advantageous to set the desorber temperature at the lower bound of the feasible region. The design space will clearly focus around 200 degrees and below.

5.2.2.3 Absorber

The tradeoff study for the absorber showed that EES would converge while the absorber temperature was within a range of 65 to 80. Figures 14 and 15 show the tradeoff studies for the absorber giving system weight in grams on the left Y axis, and

CoP on the right Y axis with Figure 14 showing data for the Series configuration, and Figure 15 showing the Parallel configuration.

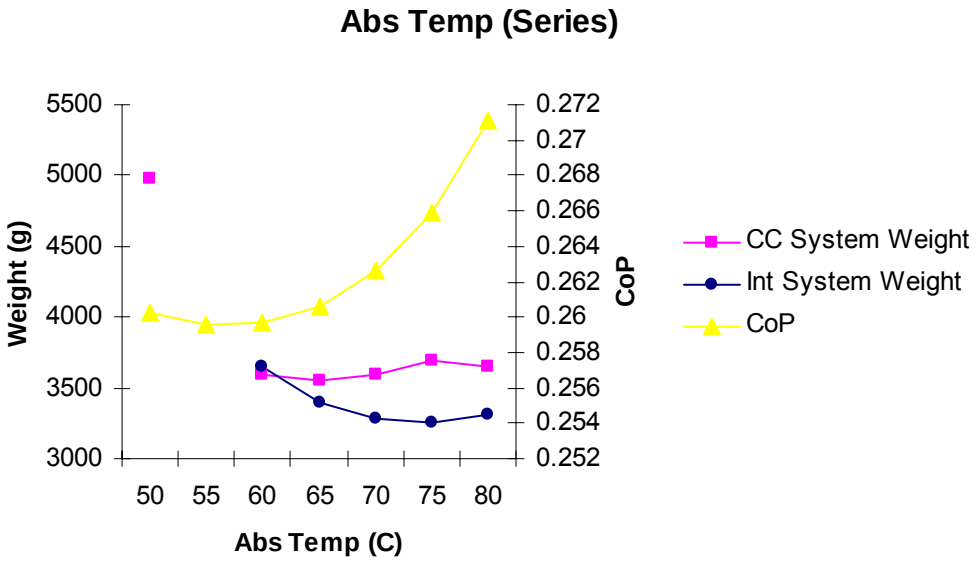

Figure 14 – Absorber Temperature (series)

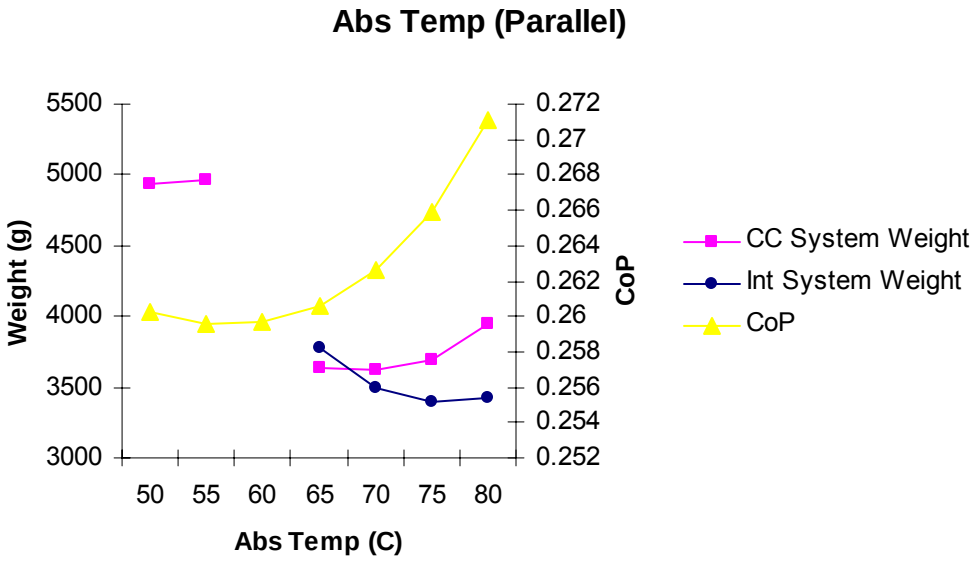

Figure 15 – Absorber Temperature (parallel)

The Absorber tradeoff study most interestingly shows a gap in the available range for analysis. The parallel configuration won't converge below 65 degrees for the interleaf geometry, and there is a gap in the channel to channel geometry between 55 and 65 degrees. If the system wouldn't converge on a solution at these points with all of the other variables at mid-level, then it is clear that it won't converge there with the other variables at extreme values, so there is a clear bottom level for the absorber temperature's design space. It makes sense that increasing the absorber temperature increases the CoP because then the desorber requires less energy from the heat source to get the fluid to the required temperature. Less energy in to the desorber means a higher CoP.

5.2.2.4 CAT

The EES thermal model is not affected by changes in the Critical Approach Temperature. The CAT is set and altered in SizingApp after the thermal model is complete; leaving the only limits to be what is physically feasible given the relative temperatures of connecting components. Therefore, the CoP is not affected by any change in the CAT. Figures 16 and 17 show the tradeoff studies for the CAT giving system weight in grams on the left Y axis, and CoP on the right Y axis with Figure 16 showing data for the Series configuration, and Figure 17 showing the Parallel configuration.

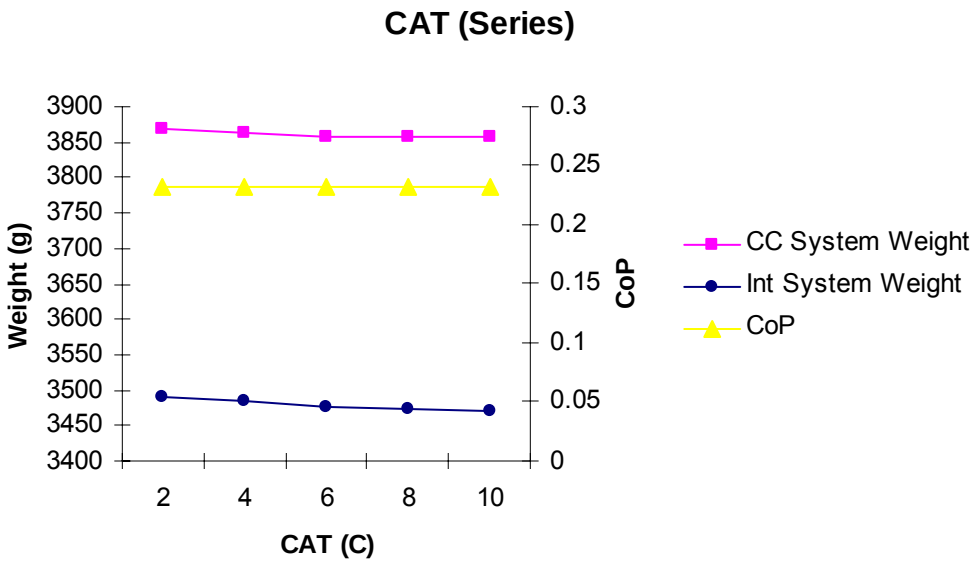

Figure 16 – Critical Approach Temperature (series)

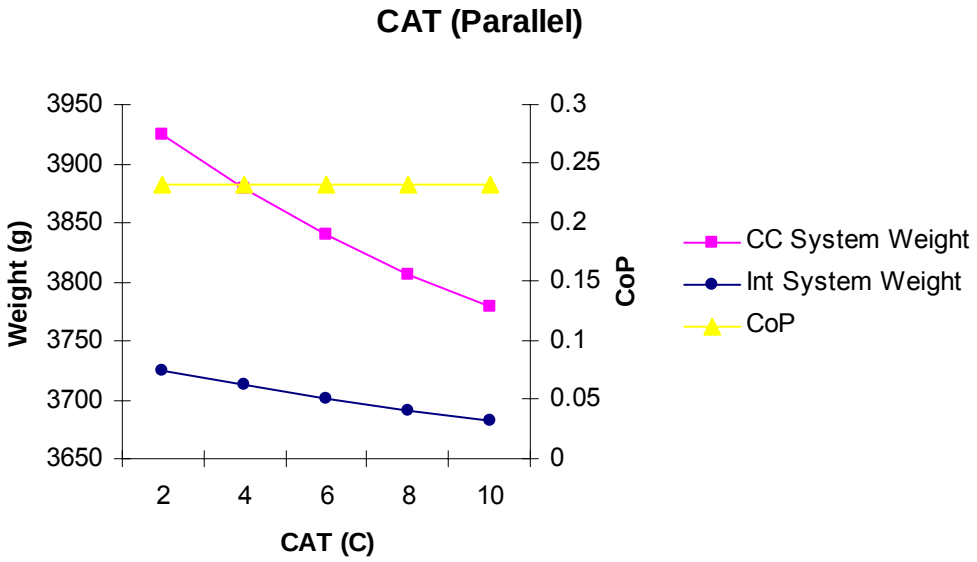

Figure 17 – Critical Approach Temperature (parallel)

It is clear that the series configuration in not affected significantly by a change in the CAT, but the parallel configuration is. This makes sense considering that the parallel configuration requires an overall temperature difference three times greater

than the series configuration because of the way the radiators are connected. With the CoP not playing into the CAT, there seems to be no reason not to push the CAT temperature difference to the larger limits since that favorably decreases the system weight.

5.2.2.5 Channel Width

The EES thermal model is not affected by changes in the channel width. The channel width is set and altered in SizingApp after the thermal model is complete; leaving the only limits to be what is physically feasible given the desired size constraints. Therefore, the CoP is not affected by any change in the channel width. Figures 18 and 19 show the tradeoff studies for the channel width giving system weight in grams on the left Y axis, and CoP on the right Y axis with Figure 18 showing data for the Series configuration, and Figure 19 showing the Parallel configuration.

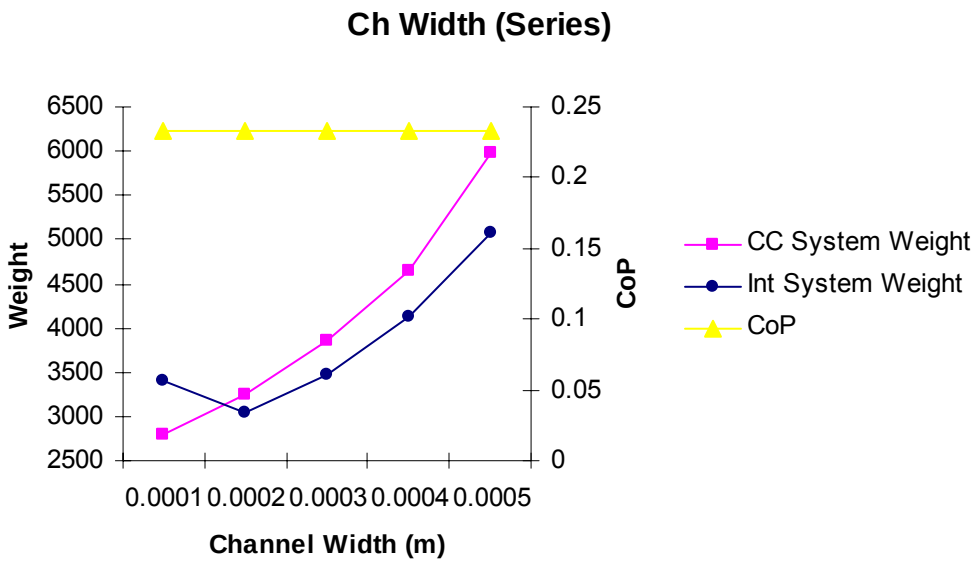

Figure 18 – Channel Width (series)

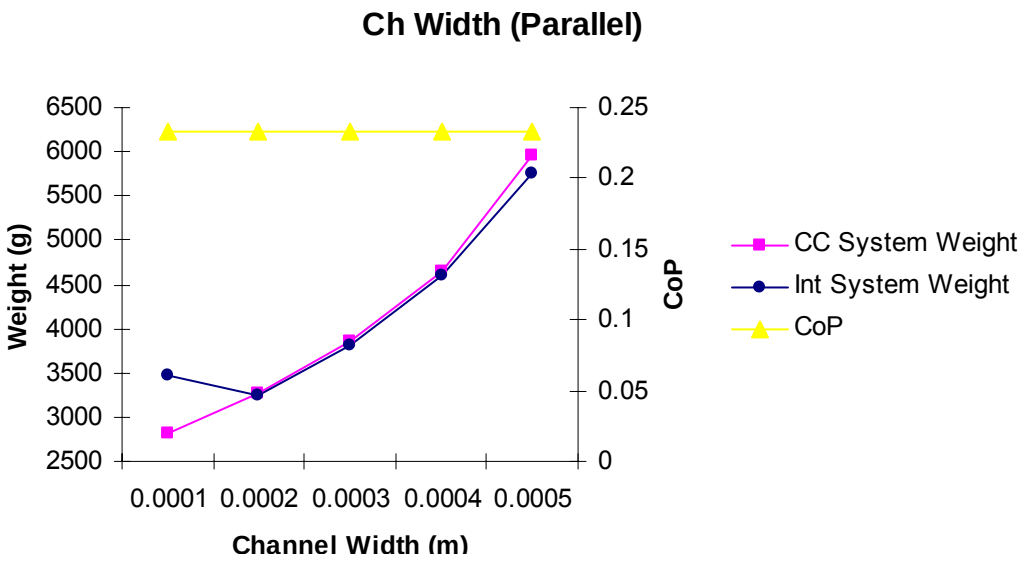

Figure 19 – Channel Width (parallel)

Both graphs from the channel width tradeoff study show the same basic trends. It seems unlikely from basic observations that 0.0005 will be used as a value for channel width, while it is clear that the design space should focus around the area of 0.0002 m, at least for the interleaf geometry. As the channel width gets larger, the overall component dimensions are also getting larger, requiring more material and increasing system weight.

5.2.2.6 Channel Length

The EES thermal model is not affected by changes in the channel length. The channel length is set and altered in SizingApp after the thermal model is complete; leaving the only limits to be what is physically feasible given the desired size constraints. Therefore, the CoP is not affected by any change in the channel length. Figures 20 and 21 show the tradeoff studies for the channel length giving system

weight in grams on the left Y axis, and CoP on the right Y axis with Figure 20 showing data for the Series configuration, and Figure 21 showing the Parallel configuration.

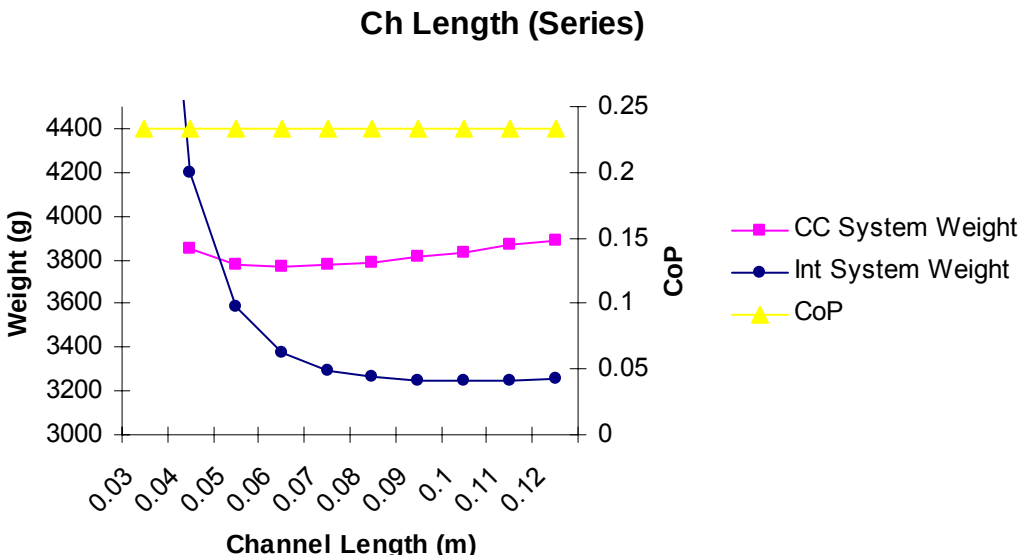

Figure 20 – Channel Length (series)

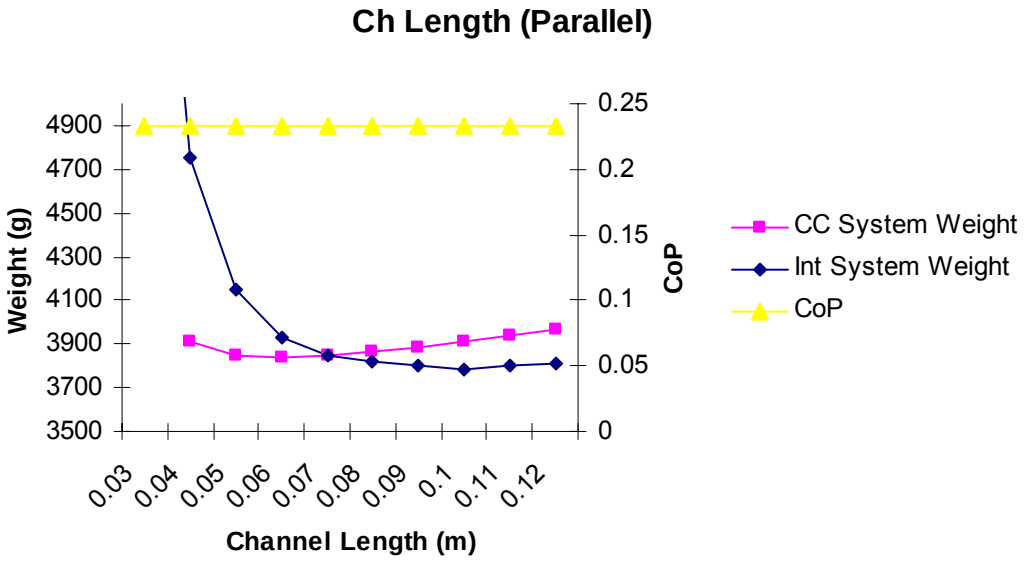

Figure 21 – Channel Length (parallel)

The channel length graphs are actually quite interesting. Channel length can be seen to have a very negligible impact on system weight as long as it stays above 0.07 m. The trend lines are not entirely flat, but channel length will most likely not be a major factor in determining optimum system weight.

5.2.2.7 Heat Exchanger T_6 (HEX)

The tradeoff study for the HEX showed that EES would converge while the T_6 was within a range of 75 to 100 degrees C. Figures 22 and 23 show the tradeoff studies for T_6 giving system weight in grams on the left Y axis, and CoP on the right Y axis with Figure 22 showing data for the Series configuration, and Figure 23 showing the Parallel configuration.

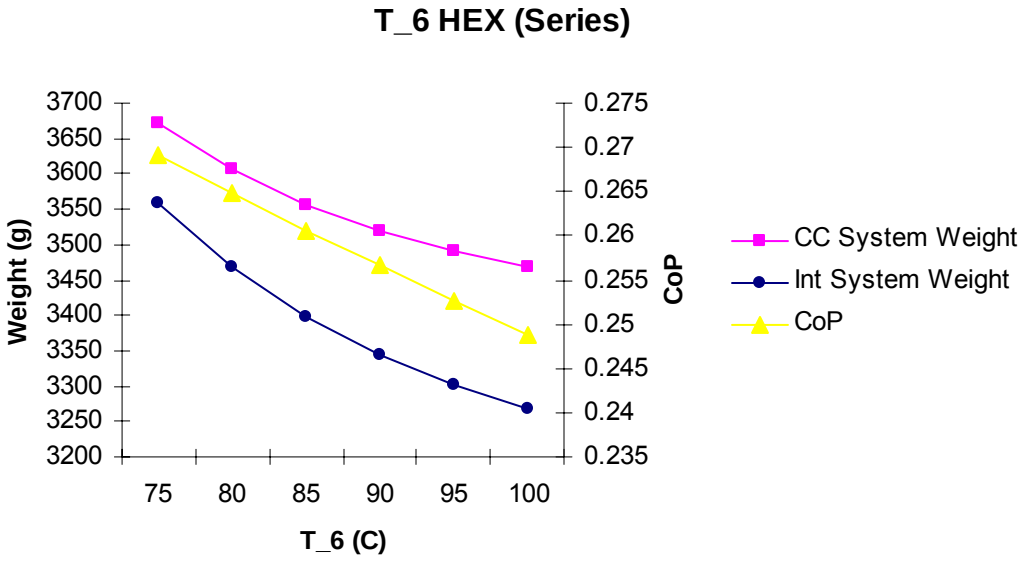

Figure 22 – Heat Exchanger Temperature (series)

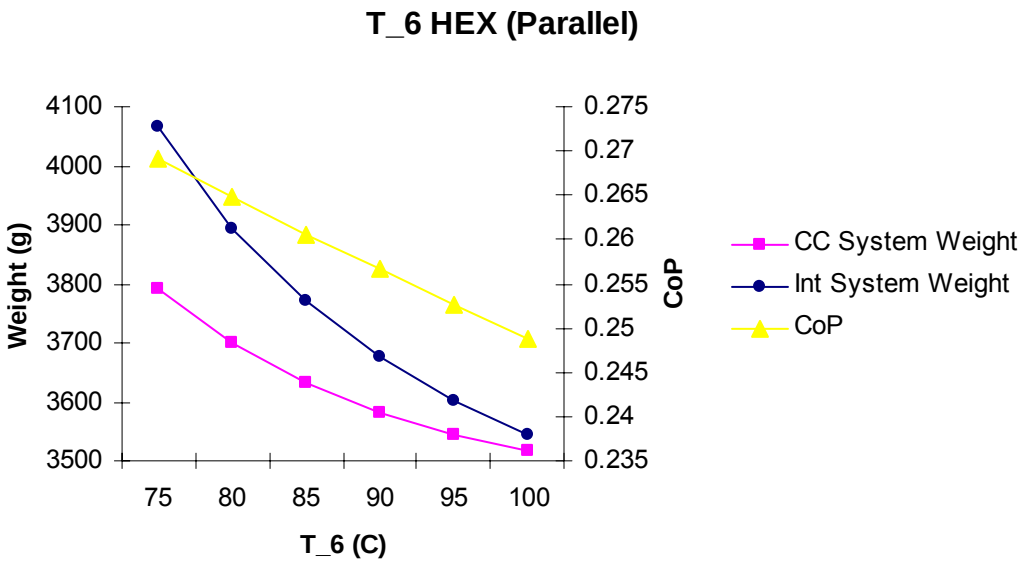

Figure 23 – Heat Exchanger Temperature (parallel)

For T_6, both graphs show the same basic trend. As the temperature of T_6 goes up, the system weight and the CoP go down. Obviously, that is not desirable, we want system weight down and CoP up, so T_6 will most likely end up somewhere in the middle of its allowable range. The CoP most likely drops as T_6 increases because it means less heat is transferred to the fluid entering the desorber, requiring a larger amount of heat input to the desorber. This does reduce the necessary size of the heat exchanger though, which reduces the weight.

5.2.2.8 Low Pressure

The tradeoff study for the low pressure showed that EES would converge while P_low was within a range of 550 to 900 kPa. Figures 24 and 25 show the tradeoff studies for P_low giving system weight in grams on the left Y axis, and CoP

on the right Y axis with Figure 24 showing data for the Series configuration, and Figure 25 showing the Parallel configuration.

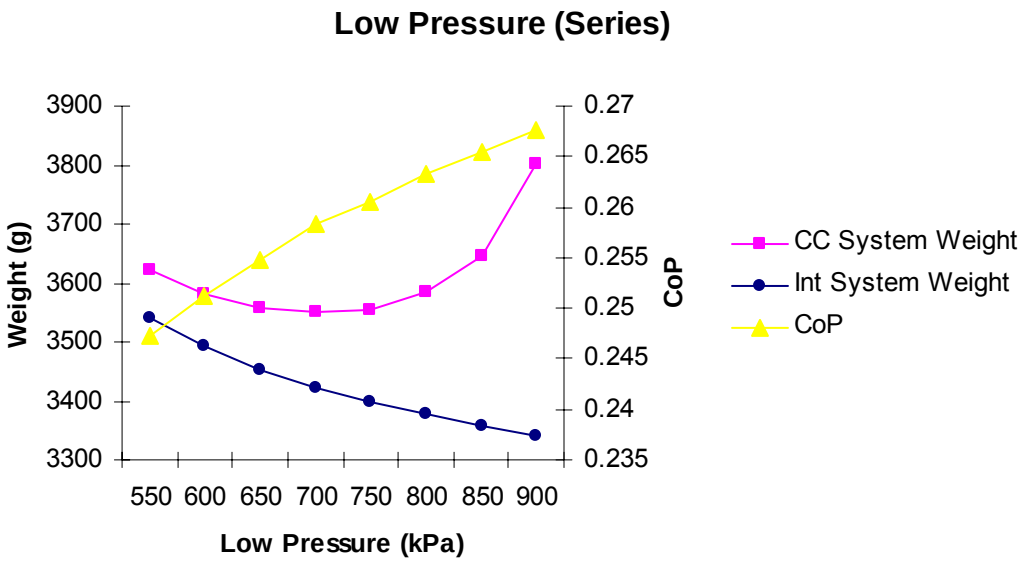

Figure 24 – Low Pressure (series)

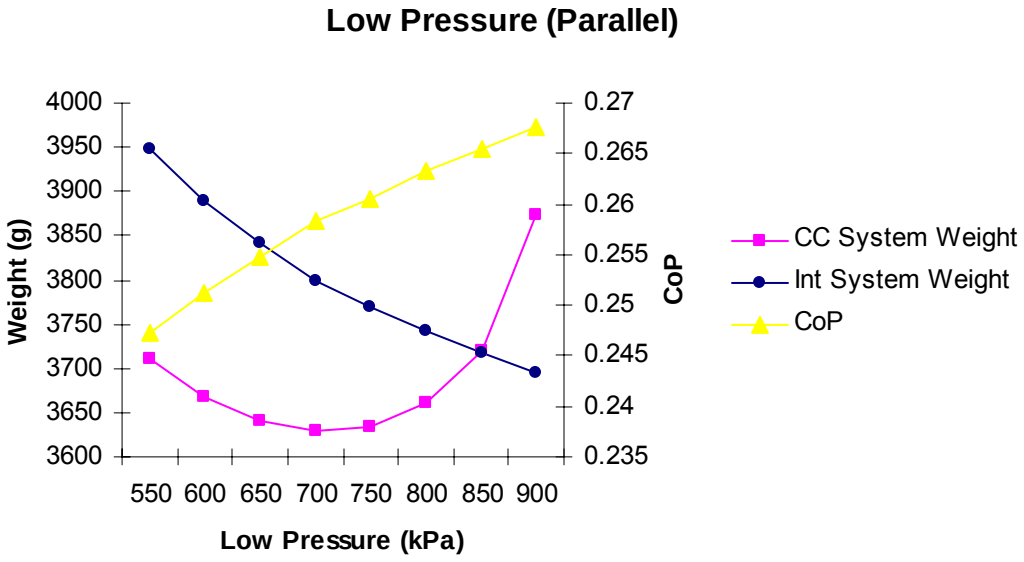

Figure 25 – Low Pressure (parallel)

These graphs show clearly that the CoP is better as the low pressure increases. The Interleaf geometry also is getting better as the upper ranges of the study area, but the channel to channel geometry shows a jump in system weight at the upper end of the study. Most likely the channel to channel and interleaf geometries will have significantly different optimal values for the low pressure.

5.2.3 Range of design variables

The tradeoff study was done changing one variable at a time while the other design variables were at mid-range values. The system will not be able to converge in some cases with all of the variables at these upper or lower ranges explored, so the design space is slightly smaller than that explored in the tradeoff study. Table 2 shows a summary of the finalized design space that was selected after evaluating the tradeoff study.

Table 2 - Finalized Design Space

Design Variable	Notation	X Representation	Range	Unit
Condenser Temp.	Tcond	X_1	60-100	deg. C
Desorber Temp.	Tdes	X_2	160-220	deg. C
Absorber Temp.	Tabs	X_3	65-85	deg. C
Critical Approach Temp.	CAT	X_4	4-10	deg. C
Channel Width	Ch_W	X_5	.0001-.0004	m
Channel Length	Ch_L	X_6	.05-.11	m
Temp. Hot out HEX	T_6	X_7	58-105	deg. C
Low Pressure	P_low	X_8	55-85	kPa/10

5.3 Surrogate Model Development

Generating an all inclusive design space for a problem with eight variables and up to five test points for each variable would create a prohibitively large number of test points. It was necessary to reduce the number of data points needed, so a standard design of experimentation (DoE) model was used to get a valid data set without running multiple thousands of simulations. This DoE is explained more fully in section 5.3.1, and the generation of a surrogate model from the data set obtained by the DoE is explained in section 5.3.2.

5.3.1 DoE Strategy for Data Collection (Sampling)

After researching multiple DoE methods in an RSM book [21] and other sources, Matlab actually provided the DoE that was used for this project. Matlab has the ability to perform D-optimal designs to generate DoE models. The user defines the number of variables, sample points, and the type of fit desired, and Matlab will output the specific configuration of cycles and points to run in order to generate a representative model. Matlab was asked to provide 180 points for the eight design variables at three levels each. The command in Matlab to generate the DoE model is shown in Equation (1).

Settings = cordexch (3, 8, 180, ‘quadratic’) (1)

This command generated a table of eight columns of 1's, -1's and 0's representing the three different levels for each variable. Table 3 shows a small portion of that table for reference.

Table 3 - Finalized Design Space

Factors:	Tcond	Tdes	Tabs	CAT	Ch_W	Ch_L	T_6	P_low
	1	-1	0	1	1	0	1	-1
	-1	0	1	-1	1	1	1	1
	1	1	1	-1	1	0	1	1
	-1	1	-1	0	1	-1	-1	-1
	1	1	-1	-1	-1	1	-1	1
	1	-1	0	1	-1	-1	-1	-1
	1	1	-1	0	-1	-1	1	0
	-1	-1	0	1	-1	0	0	1
	1	-1	-1	-1	1	-1	-1	1
	.							.
	.							.
	.							.
	.							.
	.							.
	.							.

The complete table with 180 points was then converted to show the end and mid points of the design space range, creating the table for evaluating the design space.

In addition to those points, I used my knowledge of the system and the design process to add another 50 points in areas of significant interest to provide a more exact model fit in the complicated regions. For these additional points, I also used additional levels so that most of the design variables had five different levels. This was done to ensure the accuracy of the model in the most important areas. In all, 230 different thermal configurations were processed for each physical configuration of the system (Ch-Ch, Int, Series, Parallel). For each configuration, the system weight and

CoP were recorded. Table 4 shows a sample of the complete design space table with the 1's and 0's converted to the variables' range values. Please see (C:\DocumentsandSettings\shielee\Desktop\David\ResearchProject\DesignSpace\David's Design Space.xls) for the complete data table with CoP and weight values.

Table 4 - Representation of Completed Design Space

Tcond	Tdes	Tabs	CAT	Ch_W	Ch_L	T_6	P_low
100	160	75	10	0.0004	0.08	105	550
60	190	85	4	0.0004	0.11	105	850
100	220	85	4	0.0004	0.08	105	850
60	220	65	7	0.0004	0.05	85	550
100	220	65	4	0.0001	0.11	85	850
100	160	75	10	0.0001	0.05	85	550
100	220	65	7	0.0001	0.05	105	700
60	160	75	10	0.0001	0.08	95	850
100	160	65	4	0.0004	0.05	85	850
.							.
.							.
.							.
.							.
.							.
.							.

Once the design space table was complete, each of the 230 design configurations were processed through EES and SizingApp to generate CoP and system weight values. Figure 26 shows a flow chart that summarizes the DoE and data generation procedure.

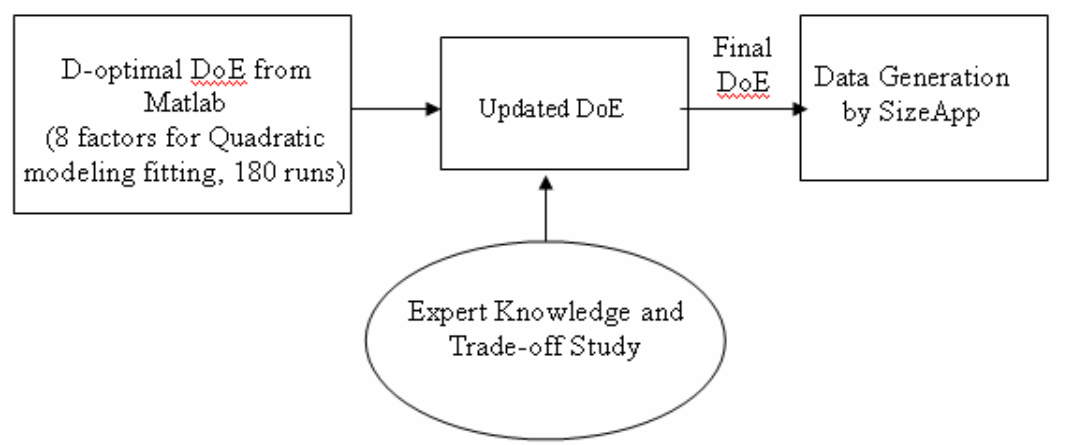

Figure 26 – DoE and Data Generation Flowchart

After SizingApp provided the system weight values for each configuration it became clear that there was no difference at all for the CoP, and minimal differences between system weights for the series and parallel radiator configurations (for reference see figures 4 and 5 in Chapter 2). Since both configurations followed the same trends, it was decided that in order to meet time constraints with the project, only one radiator configuration would be considered from this point on. After consulting Dr. Drost, the project lead here at OSU, it was determined that the parallel configuration would be the most appropriate to investigate further. At this point, the design space was complete, and the analysis moved on the generating a surrogate model.

5.3.2 Surrogate models

Once the design space was filled and all of the simulations completed, that data was evaluated using the software package S-PLUS. S-PLUS is a powerful statistical analysis program with a focus on providing a robust environment for creating

statistical applications applied to very large data sets [25]. It also has the ability to read directly from excel spreadsheets and process data in multiple ways. It was clear from the tradeoff study that a simple linear model would not give an accurate representation of the data. To be sure that an accurate model was reached, the data was initially analyzed using every quadratic and interactive term for all of the variables involved. There are two components from the S-PLUS analysis that were used to show how good of a fit the model is; the R-Squared term, and the P values. A good fitting model has an R-squared term that is close to 1, and for the individual terms, the P value should be as close to zero as possible. An individual evaluation was done for the CoP, and the Channel to Channel and Interleaf configurations. Section 5.2.2.1 will look at the CoP evaluation, and the next two sections will look at Channel to Channel and Interleaf.

5.3.2.1 CoP

The coefficient of performance is not affected by three of the variables: channel width, channel length and critical approach temperature. These three variables are adjusted and controlled in SizingApp after the thermal model is complete, and the CoP is a result of the thermal model. So the initial equation evaluated for CoP is:

$$F_{CoP} = X_1+X_2+X_3+X_4+X_5+X_6+X_1\text{^}2+X_2\text{^}2+X_3\text{^}2+X_4\text{^}2+X_5\text{^}2+X_6\text{^}2+X_1*X_2+ X_1*X_3+X_1*X_4+X_1*X_5+X_1*X_6+X_2*X_3+X_2*X_4+X_2*X_5+X_2*X_6+X_3*X_4+ X_3*X_5+X_3*X_6+X_4*X_5+X_4*X_6+X_5*X_6 \quad (2)$$

This was reduced term by term, removing the term with the highest P-value and reevaluating each time until all of the P-values were within an acceptable range (0.005 < P). The resulting equation with coefficients included is:

$$F_{CoP} = (16.7606*X_1+8.2611*X_7-1.036*X_8-0.1809*(X_1\text{^}2)-0.0242*(X_2\text{^}2)+0.0839*(X_3\text{^}2) +0.0003*(X_8\text{^}2) +0.0978*(X_1*X_2)-0.1252*(X_1*X_3)-0.0515*(X_1*X_7)+ 0.0103*(X_1*X_8)- 0.0026*(X_2*X_8)-0.0869*(X_3*X_7)+0.0061*(X_3*X_8))/1000 \quad (3)$$

This equation has a good fit because all of the P-values are within an acceptable range, and the R-squared term is 0.9909, which is very close to 1. Generally, R-squared terms around 0.90 are considered acceptable. Figures 27 and 28 show the normal and residual pot for the CoP model. The normal plot shows a good fit except for a few outliers, and the distribution of the residual plot looks fairly random, which indicates a good model.

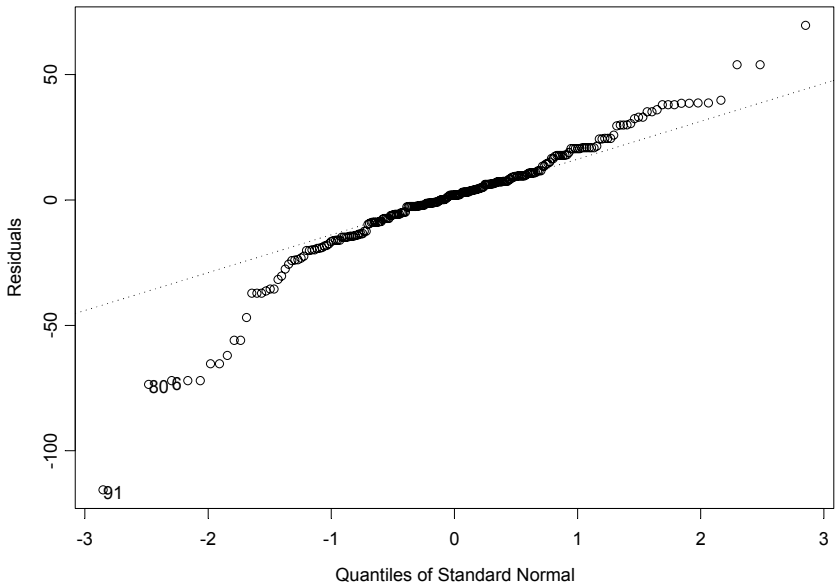

Figure 27 – Normal Plot for CoP Residuals

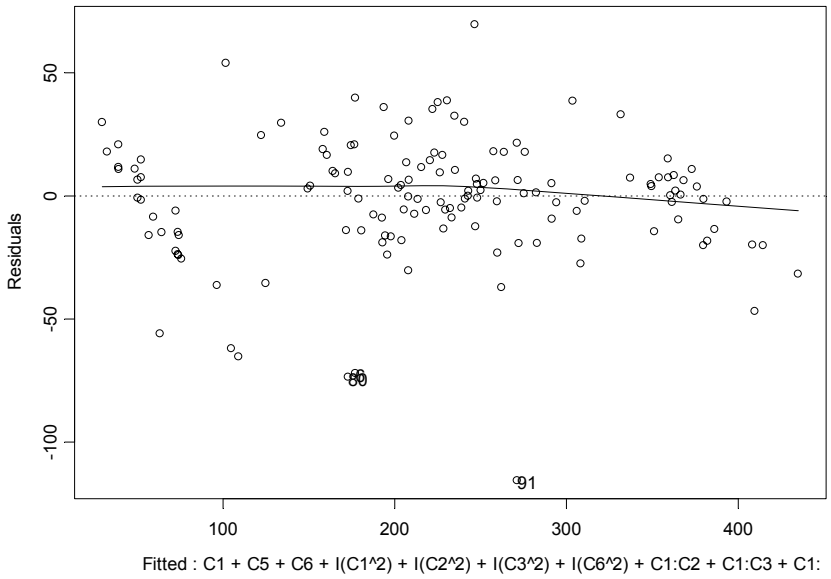

Figure 28 – Residuals Scatter Plot for CoP

From a combination of evaluating the graphs, the P-values and the R-squared term, it is clear that the model given by Equation (3) is a good fit for the CoP.

5.3.2.2 Channel to Channel

For the Channel to Channel configuration, all of the design variables were included in the initial equation. That initial equation with all of the quadratic and interactive terms is:

$$f_{Ch\text{-}Ch} = X_1+X_2+X_3+X_4+X_5+X_6+X_7+X_8+X_1\text{^}2+X_2\text{^}2+X_3\text{^}2+X_4\text{^}2+X_5\text{^}2+X_6\text{^}2+X_7\text{^}2+X_8\text{^}2$$
$$+X_1*X_2+X_1*X_3+X_1*X_4+X_1*X_5+X_1*X_6+X_1*X_7+X_1*X_8+X_2*X_3+X_2*X_4+X_2*X_5+X_2*X_6$$
$$+X_2*X_7+X_2*X_8+X_3*X_4+X_3*X_5+X_3*X_6+X_3*X_7+X_3*X_8+X_4*X_5+X_4*X_6+X_4*X_7+X_4*X_8$$
$$+X_5*X_6+X_5*X_7+X_5*X_8+X_6*X_7+X_6*X_8+X_7*X_8 \quad (4)$$

Just as with the CoP equation, Equation (4) was reduced term by term, eliminating the largest P-value term until all of the P-values were within the acceptable range. Once all of the large P-valued terms were removed, the reduced equation was:

$$f_{Ch\text{-}Ch} = -548.734*X_1-32003490*X_5+431.275*X_7+8.2631*X_8+3.2338*(X_1\text{^}2)+0.188*(X_2\text{^}2)-1.6208*(X_3\text{^}2)+26139400000*(X_5\text{^}2)-2.2863*(X_7\text{^}2)-0.6443*(X_1*X_2)+3.1433*(X_1*X_3)+121314.8*(X_1*X_5)-0.1224*(X_1*X_8)+221051.2*(X_3*X_5) \quad (5)$$

The model using Equation (5) has an R-squared term of 0.9765, and all of the P-values are actually 0.00. As with the model for CoP, Figures 29 and 30 show that the S-PLUS equation is a high-quality model. The normal values are a good fit, and the residuals are random.

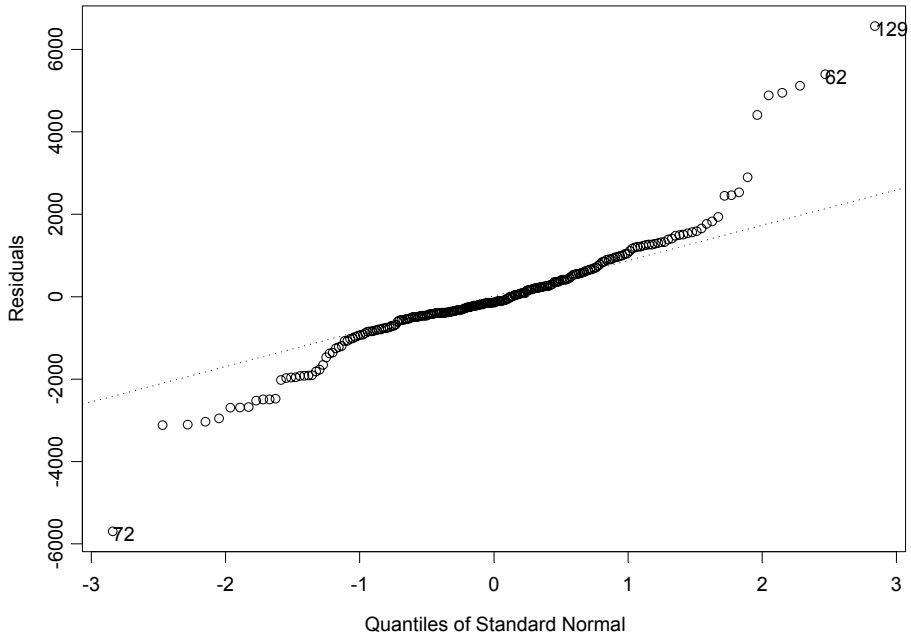

Figure 29 – Normal Residual Plot for Ch-Ch

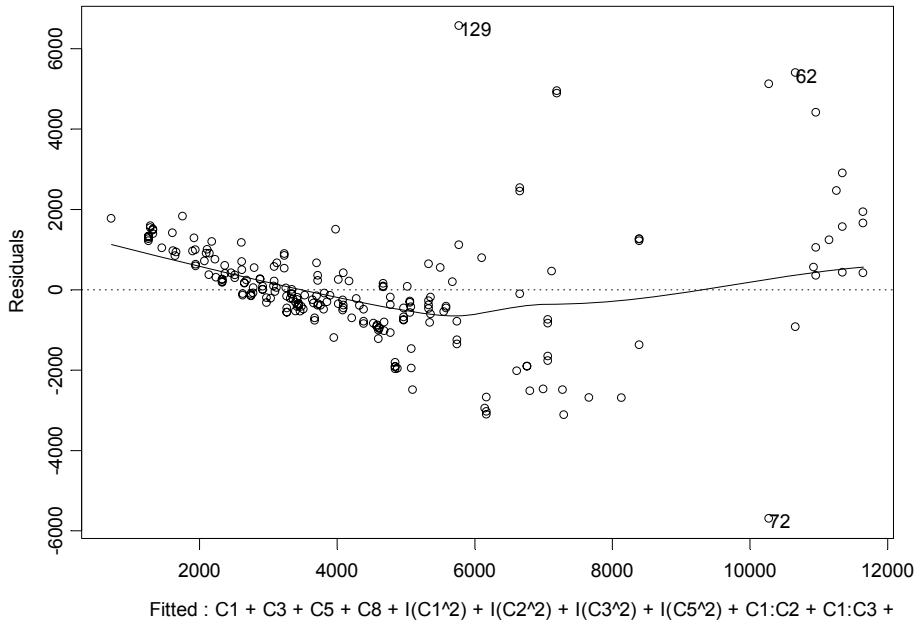

Figure 30 – Residual Scatter Plot for Ch-Ch

From a combination of evaluating the graphs, the P-values and the R-squared term, it is clear that the model given by Equation (5) is a good fit.

5.3.2.3 Interleaf

As with the Channel to Channel configuration, for the Interleaf configuration all of the design variables were included in the initial equation. That equation with all of the quadratic and interactive terms is the same as for Channel to Channel:

$$f_{Int} = X_1+X_2+X_3+X_4+X_5+X_6+X_7+X_8+X_1^2+X_2^2+X_3^2+X_4^2+X_5^2+X_6^2+X_7^2+X_8^2$$
$$+X_1*X_2+X_1*X_3+X_1*X_4+X_1*X_5+X_1*X_6+X_1*X_7+X_1*X_8+X_2*X_3+X_2*X_4+X_2*X_5+X_2*X_6$$
$$+X_2*X_7+X_2*X_8+X_3*X_4+X_3*X_5+X_3*X_6+X_3*X_7+X_3*X_8+X_4*X_5+X_4*X_6+X_4*X_7+X_4*X_8$$
$$+X_5*X_6+X_5*X_7+X_5*X_8+X_6*X_7+X_6*X_8+X_7*X_8 \quad (6)$$

Just like the CoP and Channel to Channel equations, Equation (6) was reduced term by term, eliminating the largest P-value term until all of the P-values were within the acceptable range. Once all of the large P-valued terms were removed, the reduced equation was:

$$f_{Int} = -552.2063*X_1+621.6208*X_3+3.7885*(X_1\text{^}2)-5.1785*(X_3\text{^}2)+27913840000*(X_5\text{^}2)+212504.4*(X_6\text{^}2)-0.4145*(X_1*X_2)+2.5214*(X_1*X_3)-411.42*(X_1*X_6)-0.1717*(X_1*X_8)+0.058*(X_2*X_8)-106632.8*(X_3*X_5) \quad (7)$$

The model using Equation (7) has an R-squared term of 0.9625, and the largest P-value for any of the terms is 0.0032. From Figures 31 and 32 you can see that the model for Interleaf geometry actually has the best fit from what the normal graph shows. The residuals graph also looks very good. The location of the data points seems to be completely random.

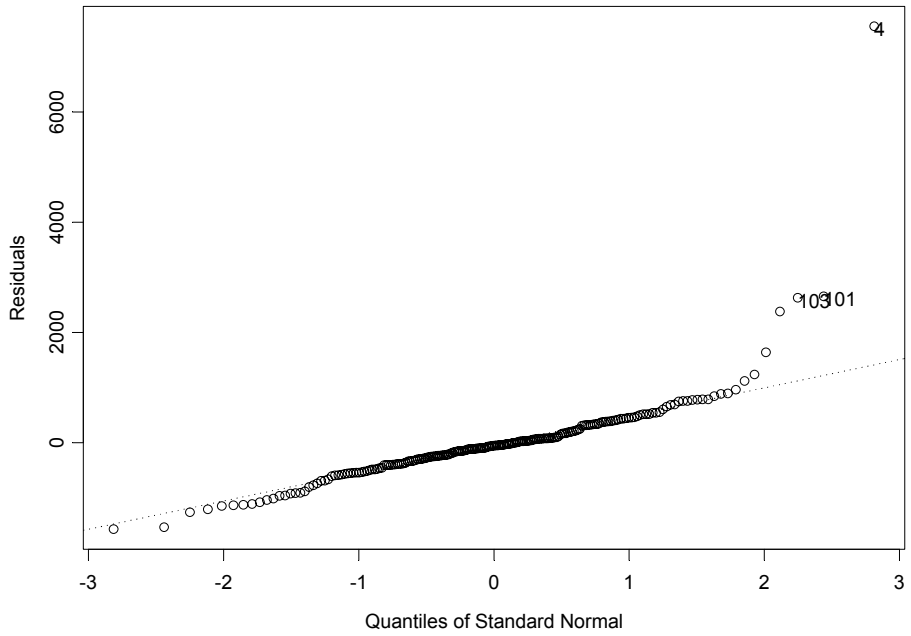

Figure 31 – Normal Residual Plot for Interleaf

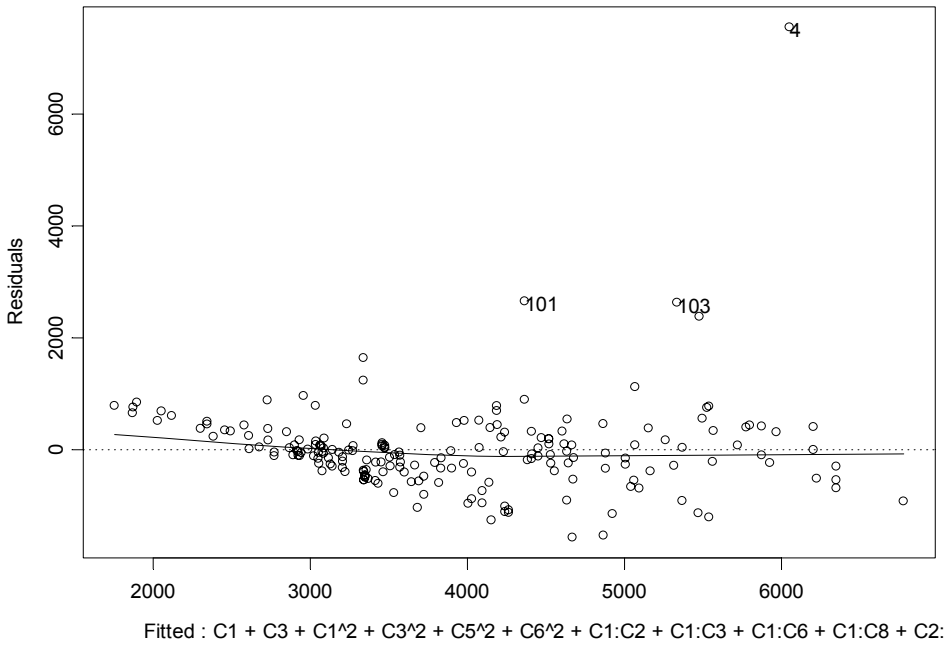

Figure 32 – Residual Scatter Plot for Interleaf

From a combination of evaluating the graphs, the P-values and the R-squared term, it is clear that the model given by Equation (7) is a good fit.

5.4 Optimization design with sensitivity consideration

5.4.1 Optimization model

After successfully generating a theoretical model of the system, it is now time to determine what configuration of component temperatures and sizes provides the best solution. The "Best" solution however is a somewhat ambiguous concept. That is where the optimization and sensitivity analysis come in. The configuration with the best coefficient of performance for the system, is not the configuration that provides minimum system weight, and vice versa. The next few sections will explain the optimization of the system and lay out the procedure for comparing unequivalent but related terms.

5.4.1.1 Objective function

The desired result is to maximize the CoP, and minimize system weight. On the most basic level, the objective function can be represented by:

$$Z\min = f_{wt}(x) + 1/\, f_{CoP}(x) \tag{8}$$

Because the CoP needs to be minimized, the function representing CoP is in the denominator of the equation.

5.4.1.2 Sensitivity Analysis

Another aspect of design being considered is the sensitivity of the system performance to change or noise. This is addressed by including a term in the objective

function that deals with the derivatives of the weight and CoP functions. By analyzing and manipulating an equation involving the derivatives, the sensitivity can be determined. So the optimal design is a combined result of optimal target performances and their robustness. Adding the term that uses the derivatives into the objective function, it now becomes:

$$Zmin = f_{wt}(x) + f(df_{wt}/dx) + 1/f_{CoP}(x) + f(df_{CoP}/dx) \quad (9)$$

To simplify the equation, each term can be represented as a Z term, so the objective function can be written as:

$$Zmin = Z_1 + Z_2 + Z_3 + Z_4 \quad (10)$$

5.4.1.3 Normalization

The CoP and system weight, as well as their derivatives, obviously do not have an equivalent magnitude, and if left as is, would have unequal effects on the objective function. That is why they need to be normalized against each other so that each has the same impact on the optimization process. This is done by dividing each component of the objective function by a value related to its overall value. This is shown below:

$$Z_1 = (f_{wt}(x) - f_{wt}(x)_{min}) / (f_{wt}(x)_{max} - f_{wt}(x)_{min}) \quad (11)$$

$$Z_2 = \sigma_F (f_{wt}(x)) / (0.2 * f_{wt}(x)) \quad (12)$$

$$Z_3 = 1 / ((f_{CoP}(x) - f_{CoP}(x)_{min}) / (f_{CoP}(x)_{max} - f_{CoP}(x)_{min})) \quad (13)$$

$$Z_4 = \sigma_F (f_{CoP}(x)) / (0.2 * f_{CoP}(x)) \quad (14)$$

Sigma (σ_F) represents the variance equation which calculates how much the system outputs change when the inputs are varied by a specific amount. In this case, the design variables' variance is set to 10 %. Equation (15) shows the base form for the variance equation.

$$\sigma_F = ((dF/dx1)^2*(\sigma_{x1})^2 + (dF/dx2)^2*(\sigma_{x2})^2 + (dF/dx3)^2*(\sigma_{x3})^2 + \ldots\ldots$$
$$\ldots+(dF/dx8)^2*(\sigma_{x8})^2)^(1/2) \quad (15)$$

Where the dF/dx terms are the partial derivatives of the weight functions with respect to the indicated variables (X_1-X_8), and the σ_x terms are the variance of the system (10%)* the X variable (X_1-X_8). For each simulation, σ_F is calculated for both system weight and CoP, and then used in the Z Equations (12) and (14).

5.4.1.4 Constraints

In order for the optimization to proceed within the working limits of the cycle, constraints need to be applied. The design variables are given upper and lower limits that fit within the design space so that the resulting optimal point is within the feasible region. Table 5 is a list of the design variable constraints, plus some additional constraints.

Table 5 - List of Constraints

Constraints
$60 \leq X_1 \leq 100$
$160 \leq X_2 \leq 220$
$60 \leq X_3 \leq 80$
$4 \leq X_4 \leq 10$
$0.0001 \leq X_5 \leq 0.0004$
$0.05 \leq X_6 \leq .11$
$85 \leq X_7 \leq 105$
$55 \leq X_8 \leq 90$
$CoP > 0.32$
$\sigma_{Weight} < 20\%$
$\sigma_{CoP} < 20\%$

The temperature constraints are taken from the range in which the thermal model can converge, and the geometric constraints result from size restrictions in the design. The last three constraints however were assigned specifically for the optimization process. The CoP constraint ensures that the system performance will be at a level of at least 0.32, and the last two constraints force the solver to find solutions in which the variance of the system is less than 20%. All of these constraints are taken into account in the optimization process.

5.4.2 Weights

One technique in multi-objective optimization involves minimizing a single equation that is the sum of positively weighted objectives. In this case there are four potential objectives: Z_1, Z_2, Z_3, and Z_4. Each objective function will be assigned a

weighting coefficient, represented by W_x, which is a fraction of one. These coefficients will add together to equal one, or symbolically, 100%. Essentially, the weighting coefficient is indicating its specific objective functions importance to the overall function as a percentage of 1. If all four Z functions were of equal importance, then the weights would be distributed as: W_1=0.25, W_2=0.25, W_3=0.25, W_4=0.25. The mathematical representation of this is shown by:

$$f(\bar{x}) = \sum_{i=1}^{k} w_i f_i(\bar{x})$$
$$where$$
$$0 \le w_i \le 1$$
$$and$$
$$\sum_{i=1}^{k} w_i = 1. \qquad (16)$$

It will be left to the user to choose what weights are appropriate for specific uses, but this study was done using five levels for each weight in each possible configuration. It is computationally time consuming, but this approach gives an idea of the shape of the Pareto surface and provides the user with information about the tradeoffs between different objectives [23]. The five levels for each weight coefficient are 0, 0.25, 0.5, 0.75, and 1. Figure 33 shows a flow chart type representation of how the coefficients could be arranged, followed by Table 6 showing all possible combinations.

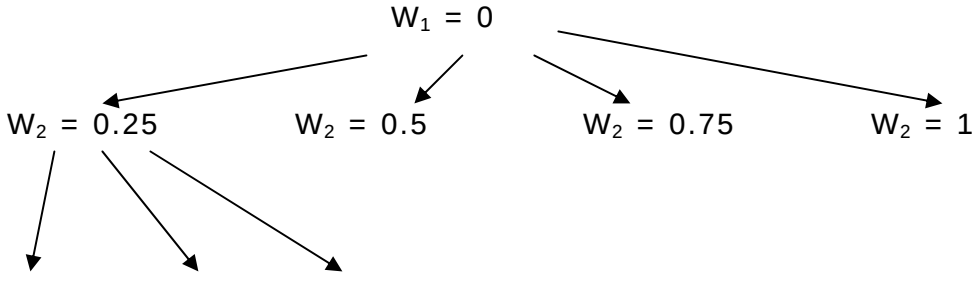

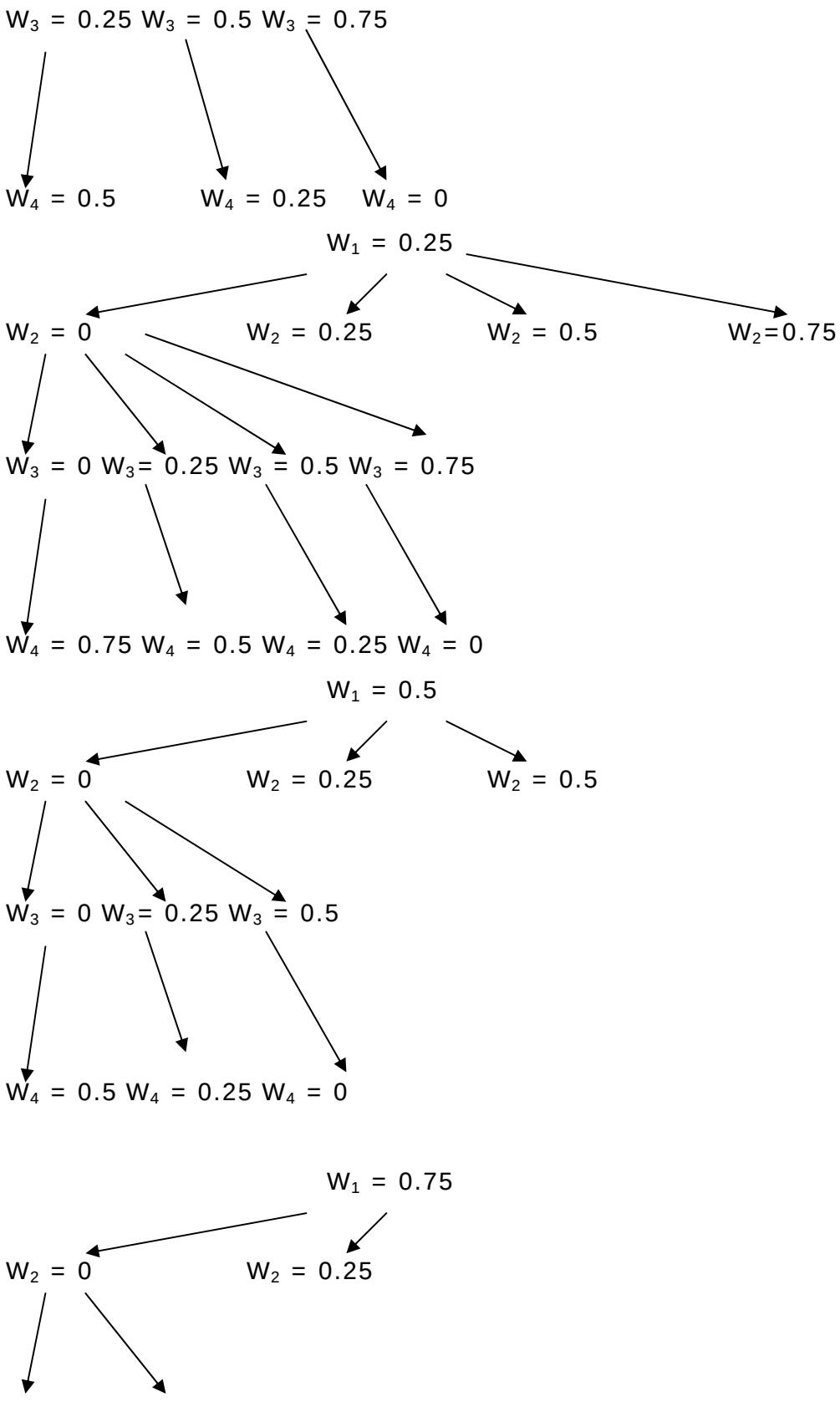
W3 = 0.25 W3 = 0.5 W3 = 0.75
W4 = 0.5 W4 = 0.25 W4 = 0
W1 = 0.25
W2 = 0 W2 = 0.25 W2 = 0.5 W2=0.75
W3 = 0 W3= 0.25 W3 = 0.5 W3 = 0.75
W4 = 0.75 W4 = 0.5 W4 = 0.25 W4 = 0
W1 = 0.5
W2 = 0 W2 = 0.25 W2 = 0.5
W3 = 0 W3= 0.25 W3 = 0.5
W4 = 0.5 W4 = 0.25 W4 = 0
W1 = 0.75
W2 = 0 W2 = 0.25

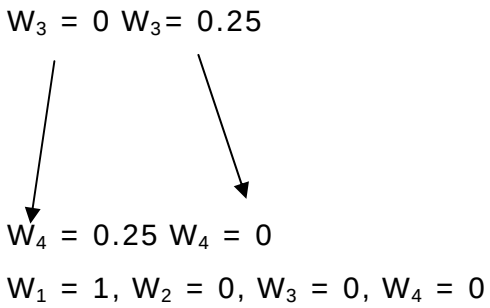

Figure 33 – Flow Chart of Potential Weight Combinations

Another way to represent the possible combinations is with a table.

Table 6 - Weight Table for Multi-Objective Optimization

Index	W_1	W_2	W_3	W_4
1	0	0	0	1
2	0	0	0.75	0.25
3	0	0	0.5	0.5
4	0	0	0.25	0.75
5	0	0	1	0
6	0	0.25	0	0.75
7	0	0.25	0.25	0.5
8	0	0.25	0.5	0.25
9	0	0.25	0.75	0
10	0	0.5	0	0.5
11	0	0.5	0.25	0.25
12	0	0.5	0.5	0
13	0	0.75	0	0.25
14	0	0.75	0.25	0
15	0	1	0	0
16	0.25	0	0	0.75
17	0.25	0	0.25	0.5

Table 6 Continued				
18	0.25	0	0.50	0.25
19	0.25	0	0.75	0
20	0.25	0.25	0	0.50
21	0.25	0.25	0.25	0.25
22	0.25	0.25	0.50	0
23	0.25	0.5	0	0.25
24	0.25	0.5	0.25	0
25	0.25	0.75	0	0
26	0.5	0	0	0.5
27	0.5	0	0.25	0.25
28	0.5	0	0.5	0
29	0.5	0.25	0	0.25
30	0.5	0.25	0.25	0
31	0.5	0.5	0	0
32	0.75	0	0	0.25
33	0.75	0	0.25	0
34	0.75	0.25	0	0
35	1	0	0	0

As can be seen from Table 6, the four coefficients with five possible weights combine for a total of 35 potential combinations. For each of these weight configurations, three starting points were tested, resulting in a total of 105 runs for both the Channel to Channel and the Interleaf configurations. With the weighting coefficients included, the main optimization function now looks like Equation (17).

$$Z_{min} = W_1*Z_1 + W_2*Z_2 + W_3*Z_3 + W_4*Z_4 \quad (17)$$

Each of these runs generated an optimal result for each design variable, and the desired outputs. These results will be discussed in section 5.4.

5.4.3 Optimization Implementation procedure

The "Solver" function from Microsoft Excel was used to process the optimization. Excel has the ability to minimize certain functions by changing specified cells, while adhering to necessary constraints. It was perfect to use for this process since it is also simple to tabulate the results after each run. The starting points and weights were in a table, and for each run, the specified row would be pasted into the target cells; then the Solver would be activated. The cell that was being minimized contained the equation for Z_{min}, Equation (17). Each of the W and Z terms are calculated from other equations programmed into the spreadsheet, based on the target cells. By changing the values in these target cells; Excel analyzes the effect certain changes have on each component of the system within the given constraints, and the overall objective function. It uses this analysis to generate an optimal solution.

5.5 Results

From the table of possible starting points and weight configurations, a range of optimal points was obtained. Below is a representative sampling of a few possible weight configuration and the optimum points that they lead to. Table 7 shows first the absolute lowest Z_{min} in the first row, and then a spread of possible weights for Channel to Channel geometry, and Table 8 shows the same for Interleaf.

Table 7 – Representative Sample of Ch-Ch Weight Combinations

Ch to Ch											
W_1	W_2	W_3	W_4	X_1*	X_2*	X_3*	X_4*	X_5*	X_6*	X_7*	X_8*
1	0	0	0	74.2	179.8	77.1	5	0.00032	0.06	91.8	64.8
0	0	0.5	0.5	66.6	160	80	6	0.0004	0.08	92.5	55
0	0.5	0	0.5	66.5	160	80	5	0.0004	0.06	92.6	55
0.25	0.25	0.25	0.25	67.1	160	80	5	0.00036	0.06	94	64.1
0.5	0	0.5	0	70.6	160	80	7	0.00027	0.1	91.1	70.3
0.5	0.5	0	0	72.8	160	80	7	0.00024	0.1	92.9	55
* indicates optimal value											

Weight *	%Wt Var.	CoP*	%CoP Var.	Zmin*
3972.28	20	0.3288	20	0.2064
4141.23	20	0.3959	13.48	0.8493
4139.57	20	0.3959	13.48	0.837
3648.49	20	0.3872	14.21	0.7321
2897.53	20	0.3694	16.66	0.5919
2938.08	17.3	0.3515	20	0.4653

Table 8 - Representative Sample of Interleaf Weight Combinations

Interleaf											
W_1	W_2	W_3	W_4	X_1*	X_2*	X_3*	X_4*	X_5*	X_6*	X_7*	X_8*
1	0	0	0	69.8	196.7	65.4	7	0.0003	0.11	95.3	74.9
0	0	0.5	0.5	61.1	160	60	5	0.0004	0.06	85	55
0	0.5	0	0.5	63.3	178.4	69.6	5	0.0004	0.05	85.7	65.1
0.25	0.25	0.25	0.25	65.2	179	61.8	5	0.0004	0.05	86	65
0.5	0	0.5	0	75.5	180.2	63	5	0.00036	0.11	87.8	65
0.5	0.5	0	0	62.8	180	74.1	5	0.0001	0.06	87.8	65.3
* indicates optimal value											

Weight *	%Wt Var.	CoP*	%CoP Var.	Zmin*
4041.96	20	0.3552	19.47	0.2343
5345.11	15.6	0.4957	8.44	0.5943
5524.79	9.31	0.4089	13.03	0.5585
5028.84	16.1	0.4373	12.3	0.6762
5106.16	20	0.3988	14.97	0.7067
3619.11	11.3	0.3893	14.25	0.3664

For both geometries, the configuration with the lowest objective function value (Z_{min}) had a weight value with $W_1 = 1$ and the rest equal to zero, so the only thing it was optimizing was the system weight. Obviously this is not an acceptable result because this is a multi-objective optimization. The actual weight percentages will most likely not be all the same as in the run with all four W = 0.25, but each of the components of the objective function are important and will most likely be included in system analysis. Table 7 and Table 8 do however show valuable information about what the system does when certain aspects are focused on. The second row of data shows where only the CoP and it's derivative are considered, and the third row shows where only the derivatives are considered, which would focus on minimizing the variance. The fifth and sixth rows show similar situations, but with the system weight and CoP being the focus.

Depending on what aspect of the objective function is emphasized through the weighting coefficients, the minimum objective function value can vary significantly. Only when the portions of the objective function that minimize the variance are ignored in the Interleaf geometry do the variance levels push up against the maximum level of twenty percent, but when those same equations are considered, the variance can drop below 10%. The amount of variance is not quite as good with the Channel to Channel geometry, with the variance only getting down to around 13.5 % at the lowest. This is still not too bad considering that the inputs are changing 10%. It is not unreasonable for the variance in system output to be only 35% larger than the variance in the inputs.

Chapter 6 Conclusions and Remarks

6.1 Summary

While the optimization process has been completed, there is still not one single correct answer to the question "What is the best configuration for a 2 kW micro-scale ammonia-water absorption cycle cooling system?" However, based on the work done here, a designer or someone planning to use this system would have a good idea on where to start. The data shows a good range of reasonable configurations for a 2 kW system that would operate within acceptable parameters. The configurations explored generate optimal system weights towards the lower end of the spectrum anywhere between 3 and 5 kg, with coefficients of performance between 0.32 and 0.4. All of these configurations also have a variance of less than 20% with a 10% change in input parameters.

It would also be possible to generate even better models to match these systems given a greater investment. The tradeoff study conducted was fairly inclusive and about as accurate as possible, but the design space only consisted of 230 points. Using the standard DoE format, 230 data points is an acceptable number of points, and as can be seen from the results of this study, are sufficient to generate a quality model. However, with more time, a more comprehensive study could be conducted using a larger data set to generate a more exact surrogate model. Also, if more time was available, a larger range of possible weight combinations could be explored to give

future designers a clearer look at how the different optimization factors interact with each other.

6.2 Future Work

When this project first began the cycle under consideration was using a load of 150 W. The cycle that was the topic of my research in this study had a load of 2 kW. I also understand that there is discussion of increasing the load even further to 5 or 6 kW. In that case, it would be necessary to conduct another study using the larger load on the system. That however is up to the people making decisions within the government.

Currently, the bench-top prototypes of the individual micro-scale components simulated in this study are in the fabrication and testing process. Once a working prototype has been completed, we will be able to compare data and results from physical tests with data from our theoretical models to verify their accuracy. Once these results are verified, the theoretical models presented here can be even more confidently used to plan and diagram system designs for various tactical energy systems, including micro-scale portable cooling systems.

7 References

[1] University of California Museum of Paleontology, http://www.ucmp.berkeley.edu/exhibits/biomes/deserts.php, Feb., 2007

[2] Daniels, B., Ballal, A., Ge, P., and Drost, K., 2004, "In Integrated Design Support Environment for a Micro-scale Portable Absorption Cooling System," *Proceedings of ASME 2004 Design Engineering Technical Conferences (DETC'04), Division of Design Automation, DETC2004-57229*, Salt Lake, Utah, 2004.

[3] Ballal, A., 2004, "Robust Design of a Micro-Scale Ammonia Absorpiton Man-Portable Cooling System", Oregon State University. Corvallis, OR

[4] Buildings Technology Center, Oakridge National Laboratory, http://www.ornl.gov/sci/btc/apps/ntrf.html, Feb., 2007

[5] Moran, M. J., Shapiro, H. N., 1999, *Fundamentals of Engineering Thermodynamics*, John Wiley and Sons, Inc., New York, NY

[6] Oregon State University, http://mecs.oregonstate.edu/, Feb., 2007

[7] Koyama, S., Kuwahara, K., and Nakashita, K. "Condensation of Refrigerant in a Multi-Port Channel". in *First International Conference on Microchannels and Minichannels*. 2003. Rochester, New York: ASME.

[8] Kim, M.H., Shin, J.S., Huh, C., and Seo, K.W. "A Study of Condensation Heat Transfer in a Single Mini-Tube and A Review of Korean Micro-and Mini-Channel Studies". in *First International Conference on Microchannels and Minichannels*. 2003. Rochester, New York: ASME.

[9] Cavallini, A., Censi, G., Del Col, D., Doretti, L., Longo, G.A., Rossetto, L., and Zilio, C. "Experimental Investigation on Condensation Heat Transfer Coefficient Inside Multi-Port Minichannels". in *First International Conference on Microchannels and Minichannels*. 2003. Rochester, New York: ASME.

[10] Steinke, M.E. and Kandlikar, S.G. "Flow boiling and pressure drop in parallel flow microchannels". in *First International conference on Microchannels and Minichannels*. 2003. Rochester, New York.

[11] Koo, J.M., Jiang, L., Zhang, L., Zhou, P., Banerjee, S.S., Kenny, T.W., Santiago, J.G., and Goodson, K.E. "Modeling of two-phase microchannel heat

sinks for VLSI chips". in *14th IEEE International Conference on Micro Electro Mechanical Systems (MEMS 2001)*. 2001. Interlaken.

[12] Zhang, L., Koo, J.M., Jaing, L., Asheghi, M., Goodson, K.E., Santiago, J.G., and Kenny, T.W., "Measurements and Modeling of Two-Phase Flow in Microchannels with Nearly Constant Heat Flux Boundary Conditions". *Journal of Microelectromechnaical Systems*, 2002. **11**(1): p. 12-19.

[13] Richter, A., Sandmaier, H., and Plettner, A. "An Electrohydrodynamic Injection Pump - a Novel Actuator for Microsystem Technology". in *Proceedings of Micro Systems Technologies 90*. 1990. Berlin.

[14] Stehr, M., Messner, S., Sandmaier, H., and Zengerle, R. "A New Micropump with Bidirectional Fluid Transport and Selfblocking Effect". in *IEEE MEMS Conference Proceedings*. 1996.

[15] Stemme, E. and Stemme, G., "A valveless Diffuser/Nozzle-Based Fluid Pump". *Sensors and Actuators; A*, 1993. **39**: p. 159-167.

[16] Zengerle, R., Kluge, S., Richter, M., and Richter, A. "Bidirectional silicon micropump". in *IEEE MEMS Conference Proceedings*. 1995.

[17] Drost, M.K., Call, C., Cuta, J., and Wegeng, R.S., "Microchannel combustor/evaporator thermal processes". *Microscale Thermophysical Engineering*, 1997. **1**: p. 321-332.

[18] Drost, M.K. and Friedrich, M. "Miniature heat pumps for portable and distributed space conditioning applications". in *Proceedings of the thirty-second Intersociety Energy Conversion Engineering Conference*. 1997. Honolulu, Hawaii.

[19] Drost, M.K., Beckette, M.R., and Wegeng, R.S., "Thermodynamic evaluation of a microscale heat pump". *Microscale Heat Transfer*, 1994. HTD - Vol. 291: p. 35-43.

[20] Munkejord, S.T., Maehlum, H.S., Zakeri, G.R., Neksa, P., and Pettersen, J., "Micro technology in heat pumping systems". *International Journal of Refrigeration*, 2002. **25**: p. 471-478.

[21] Meyers, R. H., Montgomery, D. C., 2002, *Response Surface Methodology - Process and Product Optimization Using Designed Experiments*, John Wiley and Sons, Inc., New York, NY

[22] Papalambros, P. Y., Wilde, D. J., 2000, *Principles of Optimal Design*, Cambridge University Press, New York, NY

[23] Sundaresan, S., Ishii, K., and Houser, D. (1992) Design for robustness using performance simulation programs. *Engineering Optimization.* Vol. 200

[24] McGraw Hill, Engineering Equation Solver, http://www.mhhe.com/engcs/mech/ees/whatisees.html, Feb., 2007

[25] Release Notes for S-PLUS 7 Release for Windows (April 2005)

8 Appendix A – Sample of EES Code

```
"!CALL NH3H2O(Code,In1,In2,In3: T,P,x,h,s,u,v,q)"

Load=2 [kW];        T_load=25+273.15;
T_23=T_amb;    T_24=T_load;
T_amb=50+273.15;

"T_evap=15+273.15;"
T_condin=273.15+60;
T_des=273.15+160;
T_absorb=273.15+85;
T_HEX6=273.15+105;
P_low=(1/10)*55;

T$='C:\Program Files\Xinox Software\JCreatorV3LE\MyProjects\EES
Workspace\EESSizeAppProject\Design Space File.txt'

T_condout=T_condin;    x_condin=1;    "x_condout=x_condin";    "x_12=x_condin";
"x_25=x_condin";
"x_26=x_condin";    "x_13=x_condin";  q_condin=1;    q_condout=0

"starting of code at condenser inlet"
"!condenser"
"9 - in"    CALL NH3H2O(138,T_condin,x_condin,q_condin:
T_9,P_9,x_9,h_9,s_9,u_9,v_9,q_9)
"10 - out"  CALL NH3H2O(138,T_9,x_9,q_condout:
T_10,P_10,x_10,h_10,s_10,u_10,v_10,q_10)
"2, 20 to radiator" Q_cond=m_dot_rad*SPECHEAT(Water,T=T_2,P=P_rad)*(T_20-T_2)
P_rad=4;    T_2=50+273                    "!what is P for radiator?"
h_2=ENTHALPY(Water,T=T_2,P=P_rad);    m_dot_2=m_dot_rad "defined later";    x_2=0;
P_2=P_rad;    q_2=0
h_20=ENTHALPY(Water,T=T_20,P=P_rad);    m_dot_20=m_dot_rad;    x_20=0;
P_20=P_rad;    q_20=0
-
-
-
$Export/A T$ SP7$,Type7$,Q_abs,Default,Default,Default
$Export/A T$ SP8$,Type8$,Q_rect,Default,Default,Default
$Export/A T$ SP9$,Type9$,Default,Default,Default,Default

U$='COP';    V$='CAPACITY'
cop=Q_evap/Q_des;    Q_evap=Load    "cop=m_dot_23*(h_24-h_23)/(m_dot_22*(h_5-
h_22))"

$Export/A T$
$Export/A T$ U$,V$
$Export/A T$ cop,Load
```

9 Appendix B – Changes to SizingApp Code

*This section is to document changes made to the code by David Shielee to improve
*the quality of calculations and robustness.
*the changes are marked with the line numbers that were there at the time of the change,
* and since additional changes were made above those lines, the line numbers listed are
* an approximate location, not exact in the final code

/* Changes to SizingApp.java

LINE NUMBERS	CHANGES MADE	REASON FOR CHANGE
2236,2386,2860,2861	added output lines to check values in command windows	
2864 - 2874	"[1][2]" to "[1][3]"	to output the mass in the correct column
2380 - 2383	commented out existing code and added a new line calculating Mass from volume after discussion with Dr, Ge on 09/025/2006	
2394, 2450	"comb mass" to "combined mass" to make the meaning more clear	
2863, 2872	mcomb to combinedM*1000	the variable didn't carry over from des.java and was in the wrong units
all occurences (in SizeApp)	"combM" to "combinedM" to clarify meaning of variable	
2138	added line testing for battery mass	
2874	moved totalwt to bottom of list and added line for fan	
109, 2855, 2863	initialized fanweight, set it = 500g + evapB and added it to totalwt	
110, 2856, 2863	initialized pumpweight, set it = 300g and added it to totalwt	
2137, 2195	deleted "/1000" to make evapB show up in proper units for both ch-ch and interl	
2188	capitalized from "evapweight" to "evapWeight" to maintain consistancy	
2185	Added evapL = .08 to the interleaf configuration calculations since it was missing, but was in ch-ch	
2188	deleted "double" in front of evapWeight which allowed it to show up in table	
2287	added "*1000" to condWeightField to make it print in the right units in component window	
2443	added "*1000" again to print properly in the table	
2449	also added "*1000" to combinedM for units	
2383, 2441	commented out Ashutosh's code for desWeight and replaced it with the equation that Dr. Ge and I discussed	
2393	changed the constant 650 to combinedM*1000 to reclect actual mass of peripherals	

Appendix B - Continued

To get des interleaf to work:

2412, 2413	added lines in this interleaf section that were in ch-ch for X7 and X4
2414	added desR = ... so that it didnt' equal 0 in interleaf
2438	added "desKmixH" to line to match addition in des.java

Des.java

58	added "=0" to try to make it work right
490-492	commented out Ashutosh's code, added coment and corrected mission time to reflect seconds, not hours all occurences replaced desQrate with Qdes for continuity
279, 280	commented line setting NuH constant and added line calulating it
215	added a definition in interleaf section that was missing
229, 230	I moved desL and desWi here for continuity
230	changed so that desWi = .0002, not .002
65	Removed Qdes declaration to remove error after replacing with it earlier
228	Added line desNnew = 0 to add continuity
58	commented out previous desNnew declaration
229	added "double" to make it a declaration
205	added "double desKmixH" so it would call that variable as well (also added that to lines in sizeApp where it was called 2438)

ResultTable.java

71	added line for fan and included the battery with it
66	changed "pump" to "pumps"
88	added another line to make [12]
106	added line again so that all of the needed places have the line added

*/